## A BIPOLAR PULSE TECHNIQUE FOR FAST CONDUCTANCE MEASUREMENTS

Thesis for the Degree of Ph. D. MICHIGAN STATE UNIVERSITY DONALD E. JOHNSON 1970 IHESIS



#### This is to certify that the

#### thesis entitled

A BIPOLAR PULSE TECHNIQUE FOR FAST CONDUCTANCE MEASUREMENTS

presented by

has been accepted towards fulfillment of the requirements for

Ph.D. degree in Chemistry

Major professor

Date February 27, 1970



#### ABSTRACT

## A BIPOLAR PULSE TECHNIQUE FOR FAST CONDUCTANCE MEASUREMENTS

Вy

#### Donald E. Johnson

The applications and limitations of several a-c bridge techniques and models are analyzed, especially with respect to polarization, the parallel  $(C_p)$  and series  $(C_x)$  cell capacitances, and the frequency required. A complex model of the conductance cell is developed, and the necessary experimental parameters needed in order to use a simplified model are given. It is shown that a-c techniques are accurate only over a relatively narrow frequency range. This range is especially dependent on  $C_x$  and  $C_p$  for all of the a-c bridge techniques. In the case of using a phase-angle voltmeter as a null detector, the ideal frequency is shown to be proportional to  $(C_pC_x)^{\frac{1}{1-2}}$ .

Recently, there has been considerable interest in extending conductance measurements to new areas. Several attempts to measure rapid conductance changes are cited. These techniques use unbalanced bridges and assume that any change in conductance is due purely to the resistive component. At best, this is only a very rough approximation.

Other areas of high conducta very low conducta Keasurements pecially with

overcome many niques. This secutive cons opposite pola current/volta pulse to give combines the a-c technique psec, the eff same as when slightly policis constant of is the same as

A protapplications

make accurations

1 Mohm). It

ience on Cp

titration g

output is o

there is no

on C<sub>X</sub>, where

Other areas of recent interest include solutions with very high conductance (such as molten salts) and solutions of very low conductance (such as many non-aqueous solvents). Measurements on these systems take special precautions (especially with respect to  $C_p$  and  $C_x$ ).

The bipolar pulse technique has been developed to overcome many of the limitations of the traditional techniques. This technique consists of applying two consecutive constant voltage pulses of equal magnitude but opposite polarity to a standard conductance cell. The current/voltage ratio is measured at the end of the second pulse to give the conductance directly. This technique combines the best features of both high and low frequency a-c techniques. Since the pulses can be as short as ten  $\mu sec$ , the effect on  $C_{\mathbf{x}}$  and the Faradaic impedance is the same as when using very high frequency, since  $C_{\mathbf{x}}$  is only slightly polarized. On the other hand, since the potential is constant by the end of the second pulse, the effect on C<sub>p</sub> is the same as when using very low frequency. In theory, there is no dependence on  $C_{\rm p}$  and a  $(t/R_{\rm x}C_{\rm x})^2$  dependence on  $C_x$ , where t=pulse width, and  $R_x$ =solution resistance.

A prototype instrument was built to test the theory and applications of this technique. This instrument is able to make accurate (0.01%) measurements over a wide range (100 ohm- 1 Mohm). It was found to have excellent linearity, no dependence on  $C_p$ , and only slight dependence on  $C_x$ . An acid-base titration gives a typical titration curve (continuous analog output is obtained through a sample and hold amplifier). The

rate of et
different
results by
buffered m
point chan

Ano
prototype
has a one
and the p
high abs
it has p
a narrow
dummy ar
than 0.0
0.1% at
1 kohm.
It also
and con
ments c

Since -

a Wayne

bridge

prove condit

rate of ethanolysis of acetyl chloride is studied at three different temperatures and is found to be consistant with results by others. An EDTA titration of  $Zn^{2+}$  in a highly buffered medium is followed conductometrically and an endpoint change of approximately 40 µmhos out of a total conductance of 40,000 µmhos is recorded.

Another instrument, which has many advantages over the prototype instrument, was then built. This new instrument has a one MHz crystal oscillator to control the pulse width and the pulse repetition frequency. In addition, it has a high absolute accuracy as 0.005% resistors are used. Also, it has provisions for automatic temperature compensation over a narrow (10) temperature range. Many tests have been run on dummy and real systems. It has an absolute accuracy of better than 0.05% over the range from 10 ohm to 1 Mohm, falling to 0.1% at 10 Mohm. It has a maximum sensitivity of 1 ppm at l kohm. This instrument is nearly independent of  $C_p$  and  $C_x$ . It also can be completely independent of the effects of lead and contact resistance (using a four-lead system). Measurements of solution conductances with this instrument and with a Wayne - Kerr Bridge agree within the accuracy of the bridge (0.1%).

Several applications of this technique are mentioned. Since this technique permits fast, accurate conductance measurements which are independent of  $C_{\rm x}$  and  $C_{\rm p}$ , it should prove extremely useful under a wide variety of experimental conditions.

# A BIPOLAR PULSE TECHNIQUE FOR FAST CONDUCTANCE MEASUREMENTS

Вy

Donald E. Johnson

### A THESIS

Submitted to
Michigan State University
in partial fulfillment of the requirements
for the degree of

DOCTOR OF PHILOSOPHY

Department of Chemistry

The

Professor

the online

5e

at Michi

Sharon,

especij.

Work.

#### ACKNOWLEDGMENTS

The author would like to express his appreciation to Professor C. G. Enke for his help and encouragement throughout the course of this study.

He also gratefully acknowledges a National Science
Foundation Traineeship, which supported him during his tenure
at Michigan State University.

The author wishes to give special thanks to his wife, Sharon, for all the help and encouragement she provided, and especially for typing and proof-reading the drafts of this work.

## TABLE OF CONTENTS

																					Page
I.	INT	RODUC	OITS	. 1	•	• •	•	•	•	•	•	•	•	•	•	•	•	•	•	•	1
II.	HIS	rorio	CAI, I	DEVE	ELO	PME	'nТ	OF	C	ON	טם	СT	ΆN	CE	T	EC	H	)IC	ĮĮ Į	ES	3
	Α.	D-C	Tecl	hnic	que	s.	. •	•		•	•	•	•	•		•	•	•	•	•	3
	$\mathtt{B}_{ullet}$	A-C	Tech	nnic	lue	s.	•	•	•	•	•	•	•	•	•	•	•	•	•	•	4
		1.	Trac	liti	ion	a l	Br	ide	e	Te	ch	ni	αu	es	_	•				_	4
			a.	Тур	oic	al	So	lut	io	ns	•	•	•	•	•	•	•	•	•	•	4
		_	b.	Sol	Lut	ion	IS (	of'	Hi	gh	C	on	du	ct	ì٧	it	y	•	•	•	9
		2.	Unio	que	Br	ide	e (	Гес	hn	iq	ue	S	•	•	•	•	•	•	•	•	12
		3. 4.	Phas Tecl	se-S hnic	ien Jue	sit s U	iv sec	e B d t	ri o	dg Fo	e 11	Te ow	ch C	ni	qu du	es	ar	• 1 <b>C</b> €	•	•	13
			Char	nges	3.												_	_	_		1.4
			a.	Slo	W	Cha	ng	es	•	•	•	•	•		0	•	•	•	•	•	14
			b.	Rap	oid	Ch	an,	ges	•	•	•	•	•	•	•	•	•	•	•		15
			C.	Cor	nd u	cti	vi <sup>-</sup>	ty	De	te	ct	or	S	•	•	•	•	•	•	•	16
TII.	THE	ORY (	OF A-	-C I	BRI	DGE	<b>T</b> 1	ECH	NI	QU	ES	•	•	•	•	•	•	•	•	•	18
	Α.	Gene	eral	Rri	dв	e F	'aus	ati	۸n	١											18
		Koh	rang	sch	Rr	idø	g u	Ral	an.		•	•	•	•	•	•	•	•	•	•	22
	Ċ.	Phas	se-Se	ensi	ti	AG.	De:	tec	to	r	• Ra	• 1a	nc	٥	•	•	•	•	•	•	24
	D.	App	lical	bili	ity	of	T	rad	it	io	na	1	Te	ch	ni	qυ	es	•	•	•	34
IV.	THE	BIP	OT.AR	PUI	LSE	TE	CH	NIQ	UE		•	•	•	•	•	•	•	•	•	•	37
	Α.	The	ory .			• •				•						•					37
	В.	The	oreti	ica]	E	rro	r	Ana	1 y	si	S			•	•			•	•		39
	C.	The	Inst	trun	nen	t .	•	•	•	•	•	•									40
	D.	Inst	trume	enta	11	Tes	ts	•	•	•	•	•		•		•		•		•	48
		1.	Line	eari	ity	Тe	st	•	•		•	•		•	•	•	•				48
		2.	Depe	end e	enc	e o	n I	Par	al	le	1	Сe	11	C	ap	ac	it	ar	CO	)	48
		<b>3•</b>	Depe	end e	enc	e ດ	n :	Ser	ie	S	Сe	11	C	ap	ac	it	ar	nce		•	51
		4.	A-C	Bri	dg	e C	om	par	is	on	•	•	•	•	•	•	•	•	•	•	53
	E.	Ins	trume	ent	Тe	STS	01	n C	ne	m: 1	ca	.1	Sy	's t	em	S	•	•	•	•	53
		1.	Acid	1 -	ва	se .	Ti	tra	ti	on	•	•				•	•	•	•	•	53
			Read											•		•	• .	•	•	•	56
		3.	Cond			etr	10	ED	TA	Т	it	ra	ti	on	n	f	Z j	nc	•	•	64
٧.	A N	EW II	VSTRU	JMEN	VT'	• •	•	•	•	•	•	•	•	•	•	•	•	•	•	•	70
	Α.	Impi	cover	nent	ts		•	•	•	•	•	•	•	•	•		•	•		•	70
	В.	The	New	Cir	cu	it.	•	•	•	•	•	•		•	•	•	•	•	•	•	71
		1.	Ana]	log	Ci	rcu	it	•	•	•	•	•		•	•	•	•	•	•	•	71
		2.	Digi	ita]	C	irc	ui.	t.				•						0			75

VI. C

REFERE

APPFIC

																						Page
٧.	C. D. E.	1. 2. 3. 4. 5. 6.	ain: Ab: Se: De: Ca: De: Use A-(	ingmensolnsipen penpen pencen	t ti de it de f	bso Tes vit nce anc rou dge	lud ts ccu y• or e• cor	te ura n t n S Cel	che ser	ond · · · · · · · · · · · · · · · · · · ·	uc • ar • s ad	ta • • al • Ce	.1e	el	Ce Car	el:	· · · · · · · · · · · · · · · · · · ·	tai	nec	•	•	78 82 83 83 85 86 86 86
		7•	J. 61	npe	ra	tur	e C	On	ıpe	ns	aτ	10	n	•	•	•	•	•	•	•	•	90
VI.	CON	CLUS	ION	•	•	• •	•	•	•	•	•	•	•	•	•	•	•	•	•	•	•	92
REFE	RENC	ES.	• •	•	•	• •	•	•	•	•	•	•	•	•	•	•	•	•	•	•	•	95
APPE	NDICI	ES.	• •	•	•	• •	•	•	•	•	•	•	•	•	•	•	•	•	•	•	•	99
	Α.	PROG RATI	GRAN E CC	A F	OR <b>TA</b> I	CAI NTS	LCU	LA •	TI •	NG •	• P:	SE •	UD.	00	FI •	RS	ST -	-OF	RDI	ER •	•	99
	В•	CIRC	CUIT SE C	D.	ES(	CRTI CTAI	PTI VCE	ON	о NS	F TR	IM: UM:	PR EN	OV T	ED.	) E	BIF	POI	<b>A</b> F	?	•	•	105

Table

1. C

2. F

3.

4.

5.

6.

7.

€.

9. 10.

11.

12,

13 14

A - 3

## LIST OF TABLES

Table			Page
1.	Complex Conductance Cell Symbols	•	11.
2.	Phase-Angle Voltmeter Dimensionless Parameters	•	26
3.	Examples For Using Table 2	•	28
4.	Constants for Calculating the Ideal Frequency.	•	29
5.	Phase-Angle Voltmeter Frequency Dependence	•	31
6.	Dependence on $C_x$	•	52
7•	Reaction Rate Studies Acetyl Chloride and Ethanol	0	57
8.	Absolute Accuracy Test	•	84
9•	Sensitivity vs. Resistance	•	85
10.	Dependence on C <sub>p</sub>	•	87
11.	Dependence on Series Capacitance	•	88
12.	Elimination of Contact and Lead Resistance	•	89
13.	A-C Bridge Comparison	•	89
14.	Temperature Compensation in KCl Solutions	•	91
A-1.	Three-Parameter, Least-Squares, Curve-Fit Program	•	102
A-2.	Input and Output of Least-Squares Program	•	104

## LIST OF FIGURES

Figur	e	Page
1.	A-C Conductance Bridge	, 7
2.	Complex Equivalent Circuit of Conductance Cell.	. 10
3.	A-C Bridge Analysis	20
4.	A Bipolar Pulse Conductance Device	<b>3</b> 8
5.	The Prototype Bipolar Pulse Instrument	42
6.	Timing Sequence During Measurement	44
7•	Constant Potential Generator	47
8.	Linearity Test	50
9•	Acid - Base Titration	55
10.	Reaction Rate Studies	59
11.	Temperature Dependence of Reaction Rate	61.
12.	Temperature Profile During Reaction	63
13.	Conductometric EDTA Titration of Zinc	, 66
14.	The Improved Bipolar Pulse Conductance Instrument	t 70
15.	Digital Logic Circuit for Improved Instrument .	. 77
16.	Waveforms of Logic Circuit	. 80
B-1.	Circuit Diagram of the Improved Conductance Instrument	. 106
B-2.	The Bipolar Pulse Instrument Front Panel	. 110

Con accurate

technique hasn't cl

the hist

have bee

fore acc

and the

conduct

in appl

rodel (

is val

Ine mo

tenta)

tance

in or

te d.

Simp

for

Ora;

L.C. 7

#### I. INTRODUCTION

Conductance measurement is one of the oldest of the accurate electrochemical techniques. The basic a-c bridge technique was developed nearly a hundred years ago, and hasn't changed significantly since that time. Throughout the history of conductance techniques, minor modifications have been made in the methods and the models in order to more accurately determine and characterize the conductance and the equivalent circuit of the conductance cell. The conductance techniques which are used today are quite limited in application since each was developed for a particular model of the conductance cell. The conductance measurement is valid only as long as the model truly represents the cell. The most appropriate model, in turn, depends on the experimental conditions used, especially the cell design, resistance range, and frequency.

In discussing the history of conductance techniques in Chapter II, a complex model for the conductance cell will be developed. Several examples of what has been done to simplify the cell model will be cited, and the best model for normal conductance work will be critically analyzed in Chapter III. It will be shown that the traditional Kohl-rausch method and the new phase-sensitive techniques have

very di within

especia

citano

where or ca inclu aqued molte used trad syst

0.5.6 0.5.6

read

Sev

tio

I to

it

it

w i

1=

æ

very distinct frequency ranges in which the results fall within reasonable error limits. The frequency range is especially dependent on the parallel and series cell capacitances.

Recently, there has been wide interest in systems where the traditional conductance techniques cannot be used, or can be used only with great difficulty. These systems include those with very high resistance (such as much non-aqueous work), with very low resistance (such as work in molten salts), or where platinized electrodes cannot be used (if surface adsorption is a problem). Furthermore, traditional bridge techniques are not readily applicable to systems which require continuous or instantaneous conductance measurements (such as in following conductance changes in reactions, titrations, flow systems, or ion exchange). Several attempts to measure conductance under these conditions will be cited.

A new technique, which is less restricted, will then be introduced in Chapter IV. This technique uses the best characteristics of both high and low frequency measurements. It is demonstrated on dummy and real systems and is found to be very fast, accurate, and wide-ranged. In addition, it is much simpler to use than traditional techniques as it requires no balancing (either capacitive or resistive).

Finally, a new instrument that is extremely accurate will be described. This model includes a crystal oscillator timing device, provisions to completely eliminate contact and lead resistance, and automatic temperature compensation over a narrow temperature range.

Th

compete conduction when bear of a-c ductance a constitution a constitution a trodes trodes that exhibit me

Kohlr arran hique are a betwe

to the

te at

solut

nique

### II. HISTORICAL DEVELOPMENT OF CONDUCTANCE TECHNIQUES

## A. D-C Techniques

Thus far, there has been only one technique which can compete with the a-c bridge techniques to accurately obtain conductance. This is the d-c technique, introduced by Newberry (1) in 1918. He showed some of the disadvantages of a-c methods and presented a cell arrangement for d-c conductance measurements. The d-c technique consists of applying a constant current through a cell and measuring the potential drop across a certain portion of the solution with two electrodes which carry no current. Newberry used calomel electrodes for all four electrodes, and made sure that each pair had exactly the same open circuit potential. He compared his measurements of the specific conductance of KCl solutions to those of Kohlrausch, and found the Kohlrausch values to be about 0.5% lower.

Eastman (2) extended this d-c technique and found the Kohlrausch values to be about 0.2% low. He built a bridge arrangement which could be used with either d-c or a-c techniques. He concluded that conductivities at zero frequency are about 0.02 - 0.03% higher than those at frequencies between 1 - 2 kHz. Fuoss and Kraus (3) found the d-c technique necessary for the measurement of the conductance of solutions with resistances over 100 kohm. In their

monumenta constant

100 kohm Gv

can ce :

reversi

Elias

using a

sible

tions
the p

netho

tric

ired

tech

1.

it

reg

wez

ize

W 21

monumental work to determine the influence of dielectric constant on conductance, a-c techniques were used up to 100 kohms, and d-c techniques above that value.

Cunning and Gordon (4) showed that the d-c technique can be a serious competitor to the a-c bridge techniques (0.02% accuracy). They pointed out the necessity for small, reversible electrodes, and they improved the cell design. Elias and Schiff (5) modified this technique even further by using a liquid junction to remove the measuring electrodes from the solution. This solved the problem of finding reversible electrodes for some non-aqueous solvents.

Gavis (6) rigorously derived the current-voltage relationships in d-c conductance work. He gives equations for the proper cell design, and shows under what conditions a-c methods may be used. The determining factors include dielectric constant, resistance, parallel cell capacitance, and frequency. Others (7, 8) have also had success using d-c techniques, especially with very low conductance solutions.

## B. A-C Techniques

## 1. Traditional Bridge Techniques

## a. Typical Solutions

From the very beginning of conductance measurements, it was realized that an a-c signal was necessary in order to reduce polarization of the electrodes. If a d-c potential were applied to the cell, the electrodes would become polarized, and would quickly reach a potential at which a reaction would take place (e.g. - hydrogen liberation). Applying an

a-c sign
did caus
null. Thatf-cyc
double-

recista

K

with the reactane ductane took (1) where R capacite electrone equivalent to an arms.

rausen

error

tor.

† at

a-c signal to a Wheatstone bridge with the cell in one arm did cause a problem; the bridge could not be brought to a null. The electrodes were slightly polarized during each half-cycle, giving rise to an effective capacitance (the double-layer capacitance) in series with the solution resistance.

Kohlrausch (9) was first to put a capacitor in parallel with the standard resistor in order to compensate for the reactance caused by the double layer capacitance. For conductance work prior to this, see the literature cited in his book (10). Figure 1 shows a typical conductance bridge where R<sub>X</sub> is the solution resistance, C<sub>X</sub> is  $\frac{1}{2}$  the double layer capacitance (for identical electrodes), and C<sub>p</sub> is the interelectrode and stray parallel capacitance. The Kohlrausch equivalent circuit is shown in Figure 1 with C<sub>p</sub> = 0. This method introduces a relative error of  $(R_X C_X \omega)^{-2}$ , where  $\omega$  is the angular frequency ( $2\pi f$ ), as will be shown later. Kohlrausch recommended several precautions to cut down on this error which is due to polarization of the electrodes:

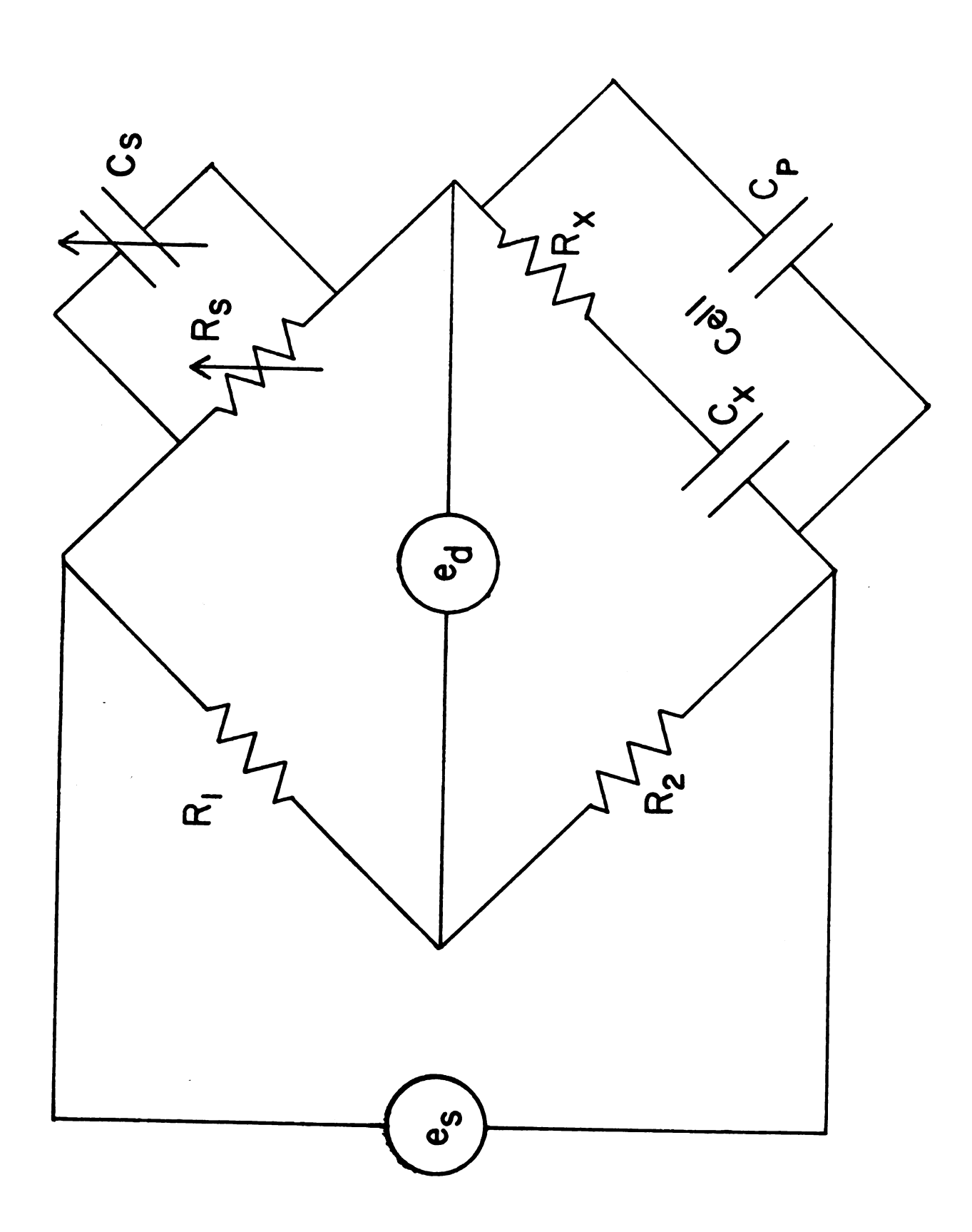
- 1) platinize the electrodes
- 2) use frequencies > 1000 Hz
- 3) use large electrodes
- 4) design the cell so that  $R_x > 100$  ohms

Washburn and Bell (11) extended the Kohlrausch method by using a "pure" signal source and a tuned telephone detector. They also stressed more careful capacitance balancing. Washburn (12) discussed the theory of cell design and showed that at high frequency,  $C_{\chi}$  can be neglected, but that

Figure 1

A-C Conductance Bridge.





parallel Atams (13 thermioni (14) also bridge to conducta to about the read Thus, t prase a two pai that th this ba

Jos

oscil rodif volta

the ch

of Tay

the ce

puttir

paral serie

pure

cell and .

rore

parallel cell capacitance causes interference. Hall and Adams (13) extended the telephone null detector by using a thermionic amplifier to increase the sensitivity. Gieringer (14) also developed an improved a-c null indicator.

Jones and Josephs (15) developed a direct-reading a-c bridge technique using a modified Wagner ground that extended conductance measurements to solutions of low conductance (up to about 60 kohm). They demonstrated that for bridge balance, the reactance in any arm must be balanced in another arm. Thus, the relationship  $R_1R_x = R_2R_s$ , is valid only if the phase angle between the voltage and current is the same in two pairs of adjacent arms of the bridge. They concluded that the method of Kohlrausch was the best approximation to this balance, and that  $R_1$  and  $R_2$  should be equal to minimize the chore of balancing reactances. They discounted the method of Taylor and Acree (16), who used an inductor in series with the cell. They also discarded as impractical the idea of putting a large capacitor in series with  $R_s$ .

Jones and Bollinger (17) made refinements in both the oscillator and detector portions of the a-c bridge. Their modifications reduced polarization because of a lower signal voltage. They were first to realize the importance of the parallel cell capacitance (18). Their model consisted of a series resistance ( $R_t$ ) and capacitance ( $C_t$ ) across a cell of pure resistance ( $R_x$ ). They were working with a capillary cell which had large filling tubes (the source of  $R_t$  and  $C_t$ ), and by its nature, a large  $R_x$ , which allowed  $C_x$  to be ignored. They used  $R_t$  and  $C_t$  to explain the Parker effect

which o constan problem imity c urement measure ideas a improve a brid

3

tist b lead a Z<sub>F</sub>, if A comp

capaci-

a simi

lent c in Tal frequ:

verse:

Werne: elimi

admit

 $tec\mu D$ 

tal c trequ which other authors (19, 20, 21) reported as a changing cell constant with increasing resistance. Their solution to this problem was to design the cell in such a way that close proximity of parts of opposite polarity would be avoided.

Shedlovsky (22) was able to obtain very accurate measurements (0.001% sensitivity) by using a screened bridge to measure conductance. Foy and Martell (23) used Shedlovsky's ideas along with suggestions by other authors to build an improved conductance bridge. Cole and Gross (24) developed a bridge that could accurately measure both conductance and capacitance over a fairly wide range. Hladek (25) designed a similar bridge (0.04% accuracy).

### b. Solutions of High Conductivity

When working with solutions of low resistance, one must be concerned not only with  $C_X$  and  $R_X$ , but also with the lead and contact resistance,  $R_C$ , and the Faradaic impedance,  $Z_F$ , if there is any possibility for a reaction to take place. A complete conductance cell can be represented by the equivalent circuit shown in Figure 2, with the symbols described in Table 1.  $Z_F$  consists of several terms, including the frequency dependent Warburg impedance (26), which varies inversely as the square root of the frequency. Winterhager and Werner (27) have used a high frequency (50 kHz) bridge to eliminate the importance of  $Z_F$ , since at high frequency, the admittance of  $C_d$  is infinite with respect to that of  $Z_F$ . No technique has been used to compensate for  $Z_F$ ; the experimental conditions are adjusted to minimize its effects (high frequency, low  $e_S$ , etc.). Feates, Ives, and Pryor (28) have

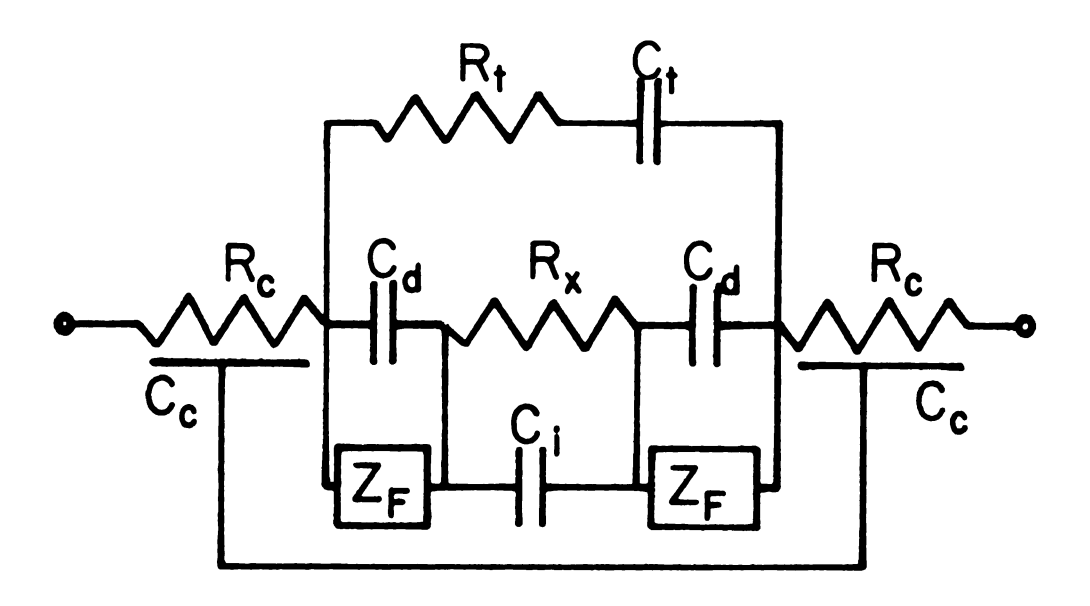


Figure 2
Complex Equivalent Circuit of Conductance Cell

Symbol	Name	Value in Simplified Model (Figure 1)
$R_{\mathbf{x}}$	solution resistance	remains the same
c <sub>d</sub>	double layer capacitance	forms $\mathtt{C}_{\mathbf{X}}$
$z_{ m F}$	Faradaic impedance	$>>$ impedance of $C_d$
$R_{\mathbf{c}}$	contact and lead resistance	reduced to zero
Cc	contact and lead capacitanc	e )
$\mathtt{c}_\mathtt{i}$	inter-electrode capacitance	combine to form Cp
$\mathtt{c}_{\mathtt{t}}$	filling tube capacitance	
$\mathtt{R}_{t}$	filling tube resistance	low or non-existent

stressed devised resistant bridge.

Wetcalf cally in that Contents that Contents and Bridge.

method
is that
for is
They p
method
(10-12)

 $c_x = 2$ 

2. <u>Un</u>

points Cruse

syste:

çzeq :

techn;

stressed the importance of eliminating  $Z_F$ . They also have devised a method to eliminate the effects of lead and contact resistance by using a special switching arrangement in their bridge. They used a four-lead, double-cell technique. Metcalf (29) points out that the double layer becomes chemically ill-defined if  $Z_F$  is important. He also points out that  $C_X$  is normally  $10^4$  -  $10^6$  times  $C_p$ . Probably the best method to date for measurements on solutions of low resistance that have low  $C_d$  is that recently developed by Robbins and Braunstein (30). They use a specially designed bridge with a series (instead of parallel)  $R_S$  and  $C_S$ , and have obtained an accuracy of better than 0.5% ( $R_X = 100$  ohm,  $C_X = 20$   $\mu F$ ).

## 2. Unique Bridge Techniques

Bertram and Cruse (31) have developed a unique R-C method for conductance measurements. The basis of the method is that the frequency and magnitude of an R-C signal generator is dependent on the characteristics of the feedback loop. They point out the frequency and sensitivity limits of their method over its entire range of conductivity measurement (10-12 - 10 ohm-1cm-1). Also, the power of this method is pointed out (32) and the method is compared to d-c methods. Cruse and Bahr (33) use the R-C method with a three-electrode system to follow reactions with half-lives of several hundred seconds.

Wershaw and Goldberg (34) used the equivalent circuit shown in Figure 1 for the cell model and devised an ingenious technique using an inductive divider bridge to obtain very

precise
variable
varied t
must be
anced pr
length o
tors mus
support
to achie
million.

conducta
technique
circuit,
electrod
ratio ar
electrod

the vers

3. Phas

applied
and McIn

compone calance

so Morm

leads.

precise measurements of conductance changes. They have a variable capacitor in each of two bridge arms which is varied to balance the reactance of  $C_{\rm p}$  or  $C_{\rm x}$ . The frequency must be varied to ensure that each cell capacitance is balanced precisely. The main disadvantage of this method is the length of time required for a measurement ( $R_{\rm s}$  and two capacitors must be balanced and the frequency varied). Strong support for the simple model is indicated, as they were able to achieve resistive balance sensitive to 0.2 parts per million.

There have been many other attempts made to obtain the conductance more easily or more accurately using a-c bridge techniques. Warshawsky (35) developed a multiple-bridge circuit. Griffiths (36, 37) developed a contactless, four-electrode system (using a three-terminal transformer as the ratio arms) that uses relatively low frequency. The four-electrode electronic half-bridge system of Ferris (38) and the very low frequency (0.8 Hz) method of Hanss and Guermon-prez (39) are just two more examples.

# 3. Phase-Sensitive Bridge Techniques

Recently, several phase-sensitive devices have been applied as null detectors in a-c bridge arrangements. Janz and McIntyre (40) used a modified impedance comparitor to separate the difference signal into in-phase and quadrature components. They were able to achieve very precise bridge balance (0.002%) over a wide resistance range (2 ohm - 20 Mohm) using an inductively coupled ratio arm and four cell leads.

observe a resistive an accura nique (42 conductor half-life

can be us
fully wifreatly :
justed i

bridge (

Sc

4. Tech

later).

a.

0f ductance

often, un to follow (such as times the Calance of

method (: with lite

differen-

lives on

Walisch and Barthel (41) have developed a technique to observe a rapid phase-shift in the difference signal near resistive balance. They claim a sensitivity of 0.0001% and an accuracy of 0.03% for their method. They used this technique (42) to follow the titration of  $Fe^{2+}$  with  $Cr_2O_7^{2-}$  conductometrically. They also studied a reaction with a half-life of approximately one minute using a self-balancing bridge (0.1% accuracy).

Schmidt (43) has shown that a phase-angle voltmeter can be used in a conductance bridge circuit quite successfully without any capacitance balancing. Although this greatly simplifies bridge balance, the frequency must be adjusted if one expects accurate results (as will be shown later).

## 4. Techniques Used to Follow Conductance Changes

## a. Slow Changes

Often, it is not necessary to know the absolute conductance, but merely to follow a change in conductance. Most often, under these circumstances, it is desirable to be able to follow the change without further manual intervention (such as balancing the capacitance and resistance). Sometimes there is time to allow semi-balance or even complete balance while following such changes. For example, Hladek's method (25) allows separate capacitance and resistance balance with little interference between them. Robertson (44) used a different method to obtain separate resistance and capacitance balance. He studied some reactions (44, 45) with half-lives on the order of 1000 secs and obtained an accuracy of

o.5% in used is identical titration the conclan improve to within

t. Si

amplifie

total) or lowing re(48) deve

able to :

acle to

short as photogra;

100 kHz s

Eur

a working kinetic r

and Lesek

for measu

a tuned a

0.5% in k (pseudo first-order rate constant). The method used is unique in that two arms of the bridge consist of identical cells: one for the reaction and the other for a titration. In this way, he could titrametrically determine the concentration vs. time. Murr and Shiner (46) developed an improved technique, and were able to obtain rate constants to within 0.03%.

### b. Rapid Changes

Sirs (47) used a 50 kHz oscillator with a rectified and amplified difference signal to obtain a d-c output. His method has an estimated relative accuracy of 5% (0.5% of total) over a 10% conductance change, and is capable of following reactions with half-lives of about 30 msec. Prince (48) developed a similar method using a 20 kHz signal and was able to follow reactions with half-lives as small as 10 msec (1 - 2% conductance accuracy). Strehlow and Wendt (49) were able to follow very fast reactions with relaxation times as short as 50 µsec, using a "pressure-step" technique. They photographed the entire relaxation curve envelope (50 or 100 kHz signal observed on the time scale of the experiment) as the system returned to bridge balance.

Eurato and Leimu (50) used a system that was based on a working curve for bridge off-balance in order to obtain kinetic results with half-lives in the seconds range. Dusek and Lesek (51) developed an improved four-electrode technique for measuring fast conductance changes. Tregloam and Laurence (52) have devised a very sensitive bridge arrangement using a tuned a-c detector followed by an a-c to d-c converter.

They ca

Ι

been mu
detecto
Conduct
tograph
conduct
They us
(55) de
detecto
determi
chromat
suggest
pecial1
bridge

 $\begin{array}{c} \textbf{A} \\ \text{in seve} \end{array}$ 

and is

as sens

changes

excelle:

His articircuits

design.

review o

They can follow a 1% conductance change within 0.5% (0.005% of total) with a response time of 1.5 msec.

## c. Conductivity Detectors

In addition to their use in kinetic studies, there has been much interest in the past few years in developing good detectors for ion-exchange and liquid-liquid chromatography. Conductivity methods have even been applied to paper chromatography (53). Duhne and Sanchez (54) developed a four-cell conductivity bridge for use as an ion-exchange detector. They used a 20 V. 20 kHz signal source. Pecsoc and Saunders (55) developed a very sensitive, low-volume conductivity detector for liquid chromatography. They used this method to determine the distribution coefficients in inorganic gel chromatography (56). Knudson, Ramaley, and Holcombe (57) suggest two circuits for general conductivity detectors (especially for chromatographic use) using operational amplifier bridge networks. One circuit is extremely sensitive (0.001%) and is linear for small changes. The other circuit is not as sensitive but is linear for even large conductance changes.

Additional information on conductance methods is given in several review articles. Gerischer (58) has written an excellent article with 203 references. He critically analyzes various bridge networks for conductance measurements. His article includes balance equations, bridge equivalent circuits, effects of  $Z_F$ ,  $C_p$ ,  $C_x$ , lead inductance, and cell design. Cruse (59) also has a very good article, with a review of the classical bridge techniques, and with special

emphasis consulted.

emphasis on high frequency methods. A review of the theory of electrolytic solutions is given by Barthel (60) with 248 references. There are also many books (61 - 64) on the subject of conductance theory and methods that can be consulted.

A content deve

cated to

fit an a

toiel is

assumes

and that

sidered

they are

When the

accurat:

Possibl.

theory

simplif

Α

work in

#### III. THEORY OF A-C BRIDGE TECHNIQUES

### A. General Bridge Equation

A complex model (Figure 2) of the conductance cell has been developed in Chapter II. This model is far too complicated to use realistically in practical applications. Therefore, the experimental parameters must be adjusted to fit an acceptable simplified model. The best simplified model is shown in the bridge network of Figure 3. This model assumes that the lead and contact resistance is negligible and that the frequency is high enough so that  $Z_{\rm F}$  can be considered infinite. These are reasonable assumptions since they are necessary conditions for accurate measurements. When the experimental parameters make this model inappropriate, accurate conductance data is extremely difficult, if not impossible, to obtain. Therefore, the following mathematical theory of a-c conductance measurements will be based on this simplified model.

Assuming a sinusoidal signal source for the bridge network in Figure 3,

 $e_s = V \sin \omega t$   $e_2 = A \sin \omega t + B \cos \omega t$ (all voltages with respect to the reference point)  $e_c = D \sin \omega t + E \cos \omega t$ 



Figure 3

A-C Bridge Analysis

Cell consists of  $R_x$ ,  $C_x$ , and  $C_p$ 

From Fig.

(A

Solving

where y

or

Ξ

If no cu  $e_1$  and e

i<sub>1</sub>

.

СЪ

cr

=

and -k

Substitut

and solvi

A =

gind n =

From Figure 3,

$$i_2 = \frac{e_2 - e_c}{R_x} = C_x \frac{de_c}{dt}$$

or (A-D)  $\sin \omega t + (B-E) \cos \omega t = R_X C_X \omega (D \cos \omega t - E \sin \omega t)$ (1)

Solving Equation 1 for D and E and letting  $K_y = \omega R_x C_y$ , where y = x, s, or p, yields:

$$D = (A + K_{y}B)/(1 + K_{y}^{2})$$
 (2)

$$E = (B - K_{x}A)/(1 + K_{x}^{2})$$
 (3)

If no current flows through the measuring device between  $\mathbf{e}_1$  and  $\mathbf{e}_2$ ,

$$i_1 + i_2 = i_3 + i_4$$

or  $C_p \omega(A\cos \omega t - B\sin \omega t) + \frac{(A-D)\sin \omega t + (B-E)\cos \omega t}{R_X}$  (5) =  $C_s \omega[(V-A)\cos \omega t + B\sin \omega t] + \frac{(V-A)\sin \omega t - B\cos \omega t}{R_S}$ 

$$\cdot \cdot K_{p}A + B-E = K_{s}(V-A) - B \frac{R_{x}}{R_{s}}$$
(6)

and 
$$-K_pB + A-D = K_sB + (V-A)\frac{R_x}{R_s}$$
 (7)

Substitution of values for D and E from Equations 2 and 3 and solving for A and B yields:

$$A = \frac{V(1 + K_x^2)(K_g Z + Y \frac{R_x}{R_g})}{Y^2 + Z^2}$$
 (8)

and 
$$B = \frac{V(1 + K_x^2)(K_s Y - Z \frac{K_x}{R_s})}{Y^2 + Z^2}$$
 (9)

wnere Y =

2 =

Let

e<sub>d</sub>

and vary

procedure

A hns

From Equ

K, and from

Substit

which :

error

in par

where Y = 
$$(1 + K_x^2) R_x/R_s + K_x^2$$

$$Z = (1 + K_x^2)(K_p + K_s) + K_x$$

## B. Kohlrausch Bridge Balance

Letting

$$e_d = e_2 - e_1 = A \sin \omega t + B \cos \omega t - \frac{V \sin \omega t}{1 + R_1/R_2}$$
 (10)

and varying R<sub>s</sub> and C<sub>s</sub> until null is obtained (the normal procedure for bridge balance) yields:

$$e_d = 0$$
 $B = 0$ 
(11)

and 
$$A = \frac{V}{1 + R_1/R_2} \tag{12}$$

From Equations 9 and 11,

$$K_{s} = (Z/Y)R_{x}/R_{s} \tag{13}$$

and from Equations 8 and 12,

$$\frac{(1 + K_x^2)(K_s^2 + Y R_x/R_s)}{Y^2 + Z^2} = \frac{1}{1 + R_1/R_2}$$
 (14)

Substitution of Equation 13 into this equation yields:

$$(1+K_x^2)(R_x/R_s)(1+R_1/R_2)$$
 Y =  $(1+R_x/R_s)$   $K_x^2$  +  $R_x/R_s$  which simplifies to:

$$\frac{R_2 R_s}{R_1 R_x} = 1 + 1/K_x^2 \tag{15}$$

Since for resistive balance,  $R_2R_s/R_1R_x=1$ , the relative error produced by balancing a bridge with a single capacitor in parallel with the variable resistor is ideally  $1/K_x^2$ , or:

$$Q = (R_{\mathbf{X}}C_{\mathbf{X}}\omega)^{-2} \tag{16}$$

For the unfavorable case of R  $_{X}$  = 200  $\Omega_{\bullet}$  and C  $_{X}$  = 10  $\mu F_{\bullet}$ 

and f = 1 kHz, the relative error is:

$$Q = (200 \times 10^{-5} \times 2\pi \times 1000)^{-2} = 0.007 = 0.7\%$$

In this example, the frequency must be at least 8 kHz in order to be within 0.01% of the correct value.

When the recommendations of Kohlrausch are followed,  $C_X$  is normally very much larger than 10  $\mu F$  for aqueous solutions. There are cases, however, especially in non-aqueous work, where the electrodes cannot be platinized. Under these circumstances,  $R_X$  must be kept large or the frequency increased in order to keep the error small. It is important to keep in mind, however, that the frequency cannot be indiscriminately increased. As soon as  $C_p$  carries significant current, the procedure for balancing out its reactance becomes very tedious, if not totally impractical. It can be seen from Equation 13 that:

$$C_s = \frac{R_x}{R_s} [(1 + K_x^2) C_p/C_x + 1] C_x/K_x^2$$
 (17)

Equation 17 can be written:

$$C_s R_s/R_x = C_p + C_x/K_x^2$$

The  $C_p$  term is usually ignored, but as the frequency is increased, the  $C_x/K_x^2$  term becomes small. As a result, the tolerances involved in adjusting  $C_s$  become small, since it now must be adjusted in the pF rather than  $\mu F$  capacitance range. It should be noted that, knowing  $C_s$  and  $\omega$ , it is possible to calculate the error term and compensate for it to obtain more accurate results. It is obvious from Equation 17 that for highly accurate results, two frequencies must be

used in order to calculate both  $C_p$  and  $C_x$ . Usually  $C_p$  is ignored, which can lead to substantial errors for high  $R_x$  and/or high frequency. It should also be noted that  $R_1$  and  $R_2$  can no longer be considered pure resistances, since at high frequencies, the small capacitances associated with them become important carriers of current.

Thus, it is evident that when using this bridge-balance procedure, one should use a compromise frequency, somewhere between the minimum frequency to be within the desired error limit and that frequency above which C<sub>p</sub> carries significant current.

### C. Phase-Sensitive Detector Balance

When a phase-angle voltmeter is used as a null detector to look at only the "in-phase" portion of the off-balance signal,  $C_s$  is not used (only  $R_s$  need be varied). From Equation 10,

$$e_{d} = (A - \frac{V}{1 + R_1/R_2} \sin \omega t + B \cos \omega t$$
 (18)

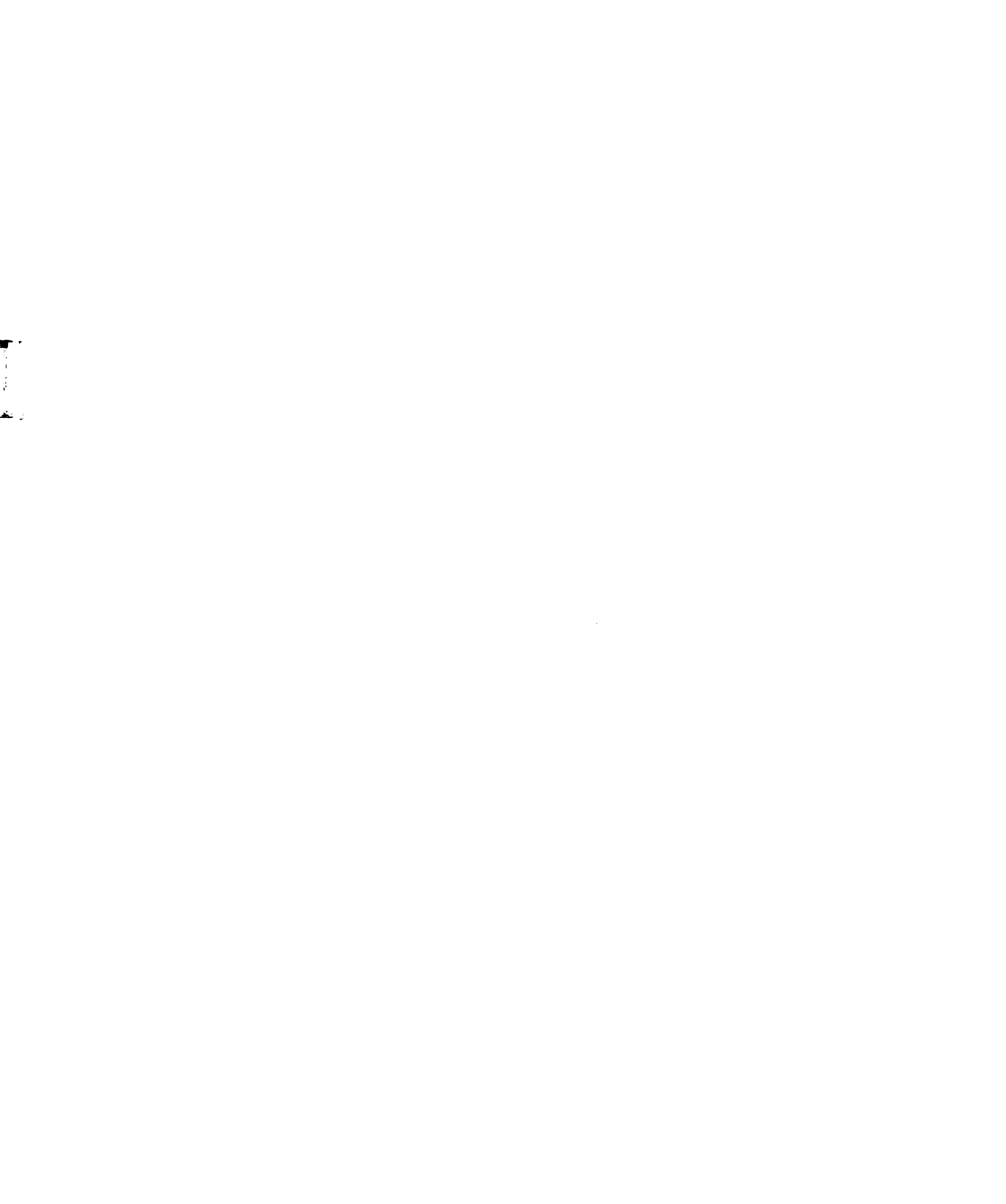
Letting  $e_d = X \sin(\omega t + \theta)$ , where  $\theta$  is the phase angle between  $e_s$  and  $e_d$ , then

 $e_d = X \cos \theta \sin \omega t + X \sin \theta \cos \omega t$ 

and 
$$B = X \sin \theta$$
 (20)

Therefore,

$$\cot \theta = \frac{A - \frac{V}{1 + R_1/R_2}}{B}$$



or Cot 
$$\theta = \frac{(Y^2 + Z^2)/(1 + R_1/R_2) - (1 + K_x^2)(R_x/R_s)Y}{(1 + K_x^2) Z R_x/R_s}$$
 (21)

Balancing out the "in-phase" portion of  $e_d$  means that the phase angle is  $90^{\circ}$ . Therefore, Cot  $\theta = 0$ , and

$$(1 + K_x^2) Y R_x/R_s = \frac{Y^2 + Z^2}{1 + R_1/R_2}$$
 (22)

This can be rewritten in terms of the relative deviation from resistance balance, Q, where

$$Q = R_1 R_x / R_2 R_s -1$$

Then Equation 22 becomes

$$(1+K_x^2)(1+Q)^2 R_2/R_1 + K_x^2(1+Q)(1-R_2/R_1) = \frac{K_x^2+Z^2}{1+K_x^2}$$
 (23)

For exact resistive balance, Q = 0, and Equation 23 becomes:

$$R_2/R_1 = K_x^2(C_p/C_x)[(1 + K_x^2) C_p/C_x + 2]$$
 (24)

or 
$$K_{x} = \left\{ \frac{C_{p}/C_{x} + 2}{2 C_{p}/C_{x}} \left[ \left( 1 + \frac{4 R_{2}/R_{1}}{(C_{p}/C_{x} + 2)^{2}} \right)^{\frac{1}{2}} - 1 \right] \right\}^{\frac{1}{2}}$$
 (25)

If 2 >>  $C_{p}/C_{x}$ , this becomes

$$K_x = (C_x/C_p)[(1 + R_2/R_1)^{\frac{1}{2}} - 1]^{\frac{1}{2}}$$
 (26)

Equation 23 can be rearranged to get:

$$K_{x}^{4}(C_{p}/C_{x})^{2} + K_{x}^{2}[(C_{p}/C_{x})^{2} + 2C_{p}/C_{x} - Q(1+R_{2}/R_{1}+Q R_{2}/R_{1})] - (1+Q)^{2} R_{2}/R_{1} = 0$$
(27)

which is quadratic in  $K_x^2$ . Table 2 shows  $K_x$  as a function of  $R_2/R_1$ ,  $C_x/C_p$ , and Q. The estimated value of  $K_x$  is calculated using Equation 26, the exact value using Equation 25, and the  $K_x$  for the errors indicated using Equation 27. Two

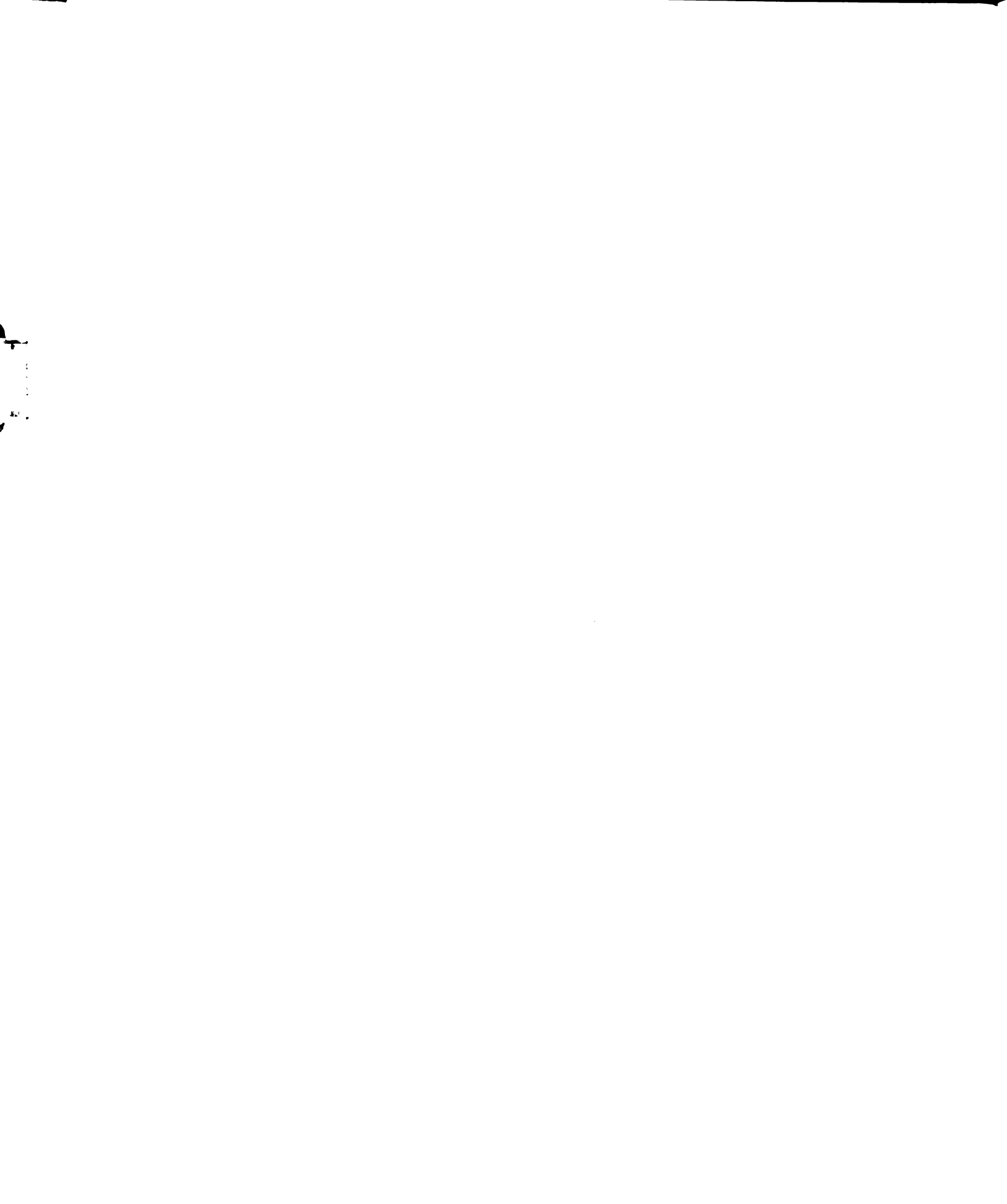


TABLE 2

Phase-Angle Voltmeter Dimensionless Parameters

	Į.			Log	; (K <sub>X</sub> )		
$R_2/R_1$	c X C	Est.	Exact	-0.1%	+0.1%	-0.01%	+0.01%
0 0	000	8489	8489 3489	4581	4542	7604	.0000
00.01	7.000	1.84894	1.84893	0.49737	4.50173	0.99737	5.00173
,	00	3442	3445	9454	4774	2520,4428	.5000
0.10	2000	$\omega$	2.34425	0.97850	4.52032	1.47535	4.01672
0 0	00	8086	.8086	.3279	6284	.6864	.0000
000	, o o o	2.80861 3.30861	2.80861 3.30861	1.34894	4.65041	1.84729 1.84924 1.84924	4.14835 5.15031
00	00	1824	.1824	4749	.0171	.9311	.5000
1000	.000	3.18243	3.68243	1.47903	5.02086	1.97889	4.52032
100.0	4 500	2.47832	2.97832	1.49719	3.50197	1.99154	3.00002
000		.9783	.9783	.4976 .4976	.5023 .5023	.9978	.0021

examples will serve to illustrate the use of the table. Assume that the double layer capacitance of each of two cells is 20 µF (C<sub>x</sub> = 10 µF) and the parallel capacitance is 100 pF. The resistance of one is 200 ohm and that of the other is 500 kohm. Table 3 shows the frequency range for desired tolerances. From these two examples, it can be seen that there is a considerable frequency range that can be used. In this case, however, the same frequency could not be used on the two cells to obtain even 0.1% accuracy.

There are two sources of deviation from the actual conductance. At high frequencies,  $C_{\chi}$  acts as a nearly perfect shunt, so that the only significant error is the positive conductance deviation caused by the shunting capability of  $C_{p}$ . At low frequencies,  $C_{p}$  carries insignificant current, and the only significant error is the negative deviation due to the impedance of  $C_{\chi}$ . Thus, to be within a desired error limit,  $\pm Q_{max}$ , the frequency should be adjusted so that:

$$\frac{\left[Q_{\text{max}}(1 + R_{1}/R_{2})\right]^{-\frac{1}{2}}}{(2\pi R_{x}C_{x})} \leq f \leq \frac{\left[Q_{\text{max}}(1 + R_{2}/R_{1})\right]^{\frac{1}{2}}}{(2\pi R_{s}C_{p}R_{2}/R_{1})}$$
(28)

Since the difference between the  $K_{\chi}$  calculated from Equations 25 and 26 is extremely small, we can write:

$$2\pi R_{x}C_{x}f = (C_{x}/C_{p})^{\frac{1}{2}}[(1 + R_{2}/R_{1})^{\frac{1}{2}} - 1]^{\frac{1}{2}}$$
 (29)

or 
$$f' = \frac{G(R_2/R_1)}{R_s(C_pC_x)^{\frac{1}{2}}}$$
 (30)

where 
$$G(R_2/R_1) = \frac{\left[\left(1 + R_2/R_1\right)^{\frac{1}{2}} - 1\right]^{\frac{1}{2}}}{2 R_2/R_1}$$
 (31)

TABLE 3
Examples for Using Table 2

Error Tolerance	$R_{x} = 20$	o Ω, R <sub>2</sub> /R	= 0.1	R <sub>x</sub> - 50	ο ka, R <sub>2</sub> /	/R <sub>1</sub> - 10
ToTerance	log K <sub>x</sub>	K <sub>x</sub>	f(kHz)	log K	Kx	f(Hz)
<b>-</b> 0 • J.	0.97	9•3	0.74	1.49	30	0.96
-0.01	1.44	27	2.2	1.98	94	3.0
0	1.84	69	5•5	2.68	480	15
+0.01	2.98	960	76	3.52	3,300	105
+0.1	3.52	3300	260	4.02	10,000	334

 $G(R_2/R_1)$  is shown in Table 4 for normal values of the ratio arm resistors.  $R_s$  is known, so that all that remains to be determined is the square root of the product of  $C_p$  and  $C_x$ . This should be nearly constant for a given cell, especially for a given solvent. Even if the product varies by two to four orders of magnitude (which is highly unlikely), the ideal frequency will only vary by one to two orders of magnitude, which normally is still within the allowed error tolerance, as indicated by Table 2.

TABLE 4

Constants for Calculating the Ideal Frequency

R <sub>2</sub> /R <sub>1</sub>	$G(R_2/R_1)$
•001	4.85
•01	1.53
•1	.480
1	.140
10	3.30x10 <sup>-2</sup>
100	6.53x10 <sup>-3</sup>
1000	1.20x10 <sup>-3</sup>

Table 5 gives some specific examples of the frequency to be used for given cell parameters. In this table,  $C_p$  is in pF, and  $C_x$  is in  $\mu$ F. The minimum and maximum frequencies indicated are for  $Q = \frac{1}{2}0.01\%$ , rigorously calculated from Equation 27. The exact and estimated frequencies are calculated from Equations 25 and 30, respectively. The next five

## TABLE 5

Phase-Angle Voltmeter Frequency Dependence

 $C_p$  in pF,  $C_x$  in  $\mu$ F' f(max) and f(min) are for  $\frac{1}{2}$ 0.01% error. The last five columns give the R<sub>s</sub> necessary for bridge balance at the indicated frequencies (0.1, 0.4, 1, 5, 10 kHz).

	01	.600	\$00 t	.000	000	. 666		496.	00	<b>&gt;</b> :	666	33.	:	•	• .	: -		_:	•	<u>:</u>	•	:	•	: .	• •	100000	1000	.666	:	7.00	• <u>0</u> 0	761.	> ~		100000	1000	00	000	.007	000	96		761	•	•
	5	039.	1035	003	7001	.000		.066	9	990	666	03.		000	1000			000	200	00	.066		· .	•		10:00:0	1001	•	000	·	000	• •			\ \ \ \ \ \ \ \ \ \ \ \ \ \ \ \ \ \ \	070	nuc.	1000		.000	÷.	.000	9	•	S. 5055
	-	919.	1597.	091.	1049.	400	1000	000	000	666	000	966	1000	010	1009	•		1000.	900.	030.	399.	000	966	1000.	• • •	1.0001	1000	000	1000	000	000	999.	900	• • • • •	٥٠	1906.	000	1000	300	10001	000	0000	999.	300	986.
	4.	374.	3025.	548.	1278.	031.	1002	0000	000	566	000	966	1000.	062	1054.			1000	0000	1000	999.	000	666	1000		100001	1000	000	1007.	000	000	999.	000			1000	000	1000	000	1000	000	900.	949.	000	999.
	۲:	7174.	530.	5973.	335.	194	1001	900	001.	000	10001	000	1000.	616	1597		005	1000	900	1000.	900	1001.		1005		1.0001	1001	000	1000	000	1000	000				1000	000	1001	000	000	000	001.	00).	. 00	307.
Ŋ	f(est)	0266.6	7.8	5724.7	5808.6	4580.8	833.3	083.3	141,2	14:1	93.0	*	70.8	1.569	9726.1	0.7/4	4 4 4 4 4 4 4 4 4 4 4 4 4 4 4 4 4 4 4 4	425.B	342.5	77.1	47.7	ţ. 4	4.0	22.4	7070.0	1572.48	540.0	458.0	83.5	08.3	14.1	4.	* *		0.7 7.087	72.6	497.2	40.6	144.0	45.5	4.2	7.7	6.7	•	C
TABLE	f(min)	6A02.1	4.60	8210.9	475.5	947.5	9.0/6	97.6	16.0	31.6		7		2.90	426.9		222.8	0.00	30.2	1.5	3.1	~	۳.	٠. ت		95.30	4.8	22.4	0.3	•	7	*; '	•	•	94		. V	Ś	2.2	9	۲,	۳.	•	•	:
	f (ex)	0266.3	7,1	5724,7	5868,5	4580.8	<b>8</b> 33,3	083.3	141,2	14.1	93,9	4.0	70,8	895.5	9725,8	017/4	1448.9	425.A	342.5	77.1	67.7	4.5	4	22.3	7020.5	1572.49	580.7	58.0	83,3	08.3	14.1	4.	•	•		71.5	497.5	48.3	•	42.6	4.2	7.7	6:7	•	7
	f (max)	04.1	3170722	07.8	12474.5	0287.4	1014.0	191.4	967.9	93.7	188.1	503.5	1591.7	47581.3	636723.3	5 · 2 / 1 / 5 / 6 / 6 / 6 / 6 / 6 / 6 / 6 / 6 / 6	7. 7. 4. 7. 4. 4. 4. 4. 4. 4. 4. 4. 4. 4. 4. 4. 4.	2405	5267.4	994.3	599.1	135. X	403.5	1591.7		166628.A3	24471.1	22487.1	2781.2	274.1	996.1	1000	0 . K . C		1991.7	A40010.R	146901.9	2507.S.A	92507.3	2780. B	978.9	196.4	590°A	45.5	
	$R_2/R_1$	0.0	7	7	٦,	Ξ	;	3		100.	000	99.	0000	•	-	•	-			90.	000	000	٠.	0000	• "				:	3	30.0	1001	٠.		50			: :		3	3	0.0	٦.	5.	0.00
	<b>∝</b> ×	100		0	2	6	8	o 0 0	1000	60	000000	0000000	0000000		<b>~</b>	= (	2 6	5	0	000	0000	000000	600	0000000				0	0	000	1000	000000	1000001	000000	1000000000				0	•	600	000	00	10:01	9000
	υ×		4				<b>→</b>	-	-				_	2	2	0;	)   	9 C	•	10	0	10		0	<b>E</b> (			C	•	€.	C	•	0	D	- - - - -		5	5		5	5	5	6	0:0	0,0
	_																																		00										

100   0.0	01	.0 14	5.3 1008.8	9666	97.63	666	.4 9663	.964 0.	.4 7085.	.3 963.	ه. م	·/e/	7000	.0666 9.	.0001 0.	R66 6.	000				400 B.	.0 /67.	.0 10n00.	1000.			.666	.8 9663.	.964	.5 7685.		.0 /67.	.0 10000.	.00 1000.	.0000		0000	.8 9663.	.966	.5 /645.	.594	
1	2	5001 5.	.6 103	.7 1000	27		.1 991	66 0.	.2 917	9.	.9 620	16 1.	1000	202 9.	.5 100	.7	•	166	7.57	)	•	-:	.1	100		656	20 0.	.4 991	66	.2	6. 6. 6. 6. 6. 6. 6. 6. 6. 6. 6. 6. 6. 6	16 1.	.0	007 0.	300 O.	001		166 4.	.0	.2 41	64 9.	
K         K	-	.5 1091	5,2 159	4.7 1908		5.7 100	666 9.6	0.1 100	3,7 . 996	6.0	7.7 963			.4 1000	100	.1 999	.1 100	•	6.7 O.		7 943	•	.6 100	9.	001		07	66 T.	01	66°	, vo	•	1000	.0 100	1000	001		900	100	966	66 6.	
K         F <sub>2</sub> /K <sub>1</sub> F(max)         F(min)         F(min) <td>7.</td> <td>9.9 14</td> <td>9.7 30</td> <td>5.0 105</td> <td></td> <td></td> <td></td> <td>1.0</td> <td>6 2.0</td> <td>0.5</td> <td>5.1 9.1</td> <td></td> <td>00<b>1</b> 702</td> <td>1.0</td> <td>0.4 10</td> <td>4.9 100</td> <td>3.9</td> <td>000</td> <td>0.00 TO</td> <td></td> <td>6.1 993</td> <td>۱.۱ وو</td> <td>0.0 1000</td> <td>0.1 100</td> <td>000</td> <td></td> <td>0.0</td> <td>0.0</td> <td>001 0.6</td> <td>9.0</td> <td>100 T.A</td> <td>0.0</td> <td>0.1 1000</td> <td>0.1 100</td> <td>1000</td> <td>001 0.0</td> <td></td> <td>0.0</td> <td>001 000</td> <td>666 9.0</td> <td>99 0.0</td> <td></td>	7.	9.9 14	9.7 30	5.0 105				1.0	6 2.0	0.5	5.1 9.1		00 <b>1</b> 702	1.0	0.4 10	4.9 100	3.9	000	0.00 TO		6.1 993	۱.۱ وو	0.0 1000	0.1 100	000		0.0	0.0	001 0.6	9.0	100 T.A	0.0	0.1 1000	0.1 100	1000	001 0.0		0.0	001 000	666 9.0	99 0.0	
1	•	.70 371	14 105	159	77		58 100	11 10	71 99	29 10	94		51 62	.48 100	.87 10	100	01 70		15		90.	.09 10	.57 100	19.	001 97	66.	.58 10	.25 100	.71 10	06 //	00	.24	.67 100	.49 10	100	60.	or re-	63 100	.41 10	.14 99	.94 10	
R	f(est)	1 1589	7 4972	497	911 9/	21 342	92 34	33 67	53 6	59 12	17	16 2	202 1972	197	56 458	76 45	67 108	01	17 06		32	32	52 <b>15</b> 8	69 497	77.	28	29 34	50	17	32	7	20	61 50	80 157	58 15			30	32 2	50	3.5	
100   10   10   10   10   10   10   1	f(min)	1 1420	7 4423	442	12303	6 2419	0 241	305	1 30	31	<b>5</b>	7 6 7 6	8210	7 421	5 2047	8 204	3 297	•	19 -	· ·	. •	•	9 110	1 942	900		8 30	9	<b>-1</b>				6 31	66 6		, ·	- T	· 10	•	•	•	
X	f (ex)	15894.	49723.7	4972,	4487	3425.7	342.5	677.1	67.7	124.9	12,4	75.4	15724.7	1572.4	4580.8	458.0	1063,3	2.001	214.1		0°P	7.0	1589.5	4972.6	407.2	8.441	342.5	34,2	67.7		2.5	2.2	505.6	1572.4	157.2			10.0	21.4	2.1	3.0	
2	f(max)	836A.4	7911.3	5701.1	760.9	213	921	590.3	150.9	503.9	5	1.961	7,0000	13377.7	0287.A	123.7	491.4	7776	) • • • • • • • • • • • • • • • • • • •			59.1	E6754.1	43A72. 3	6.787.7 2584 R	2228.4	269.5	924.0	500.	9.0	2 6	20.7	49639.9	46429.4	16462.	1./012	7.047	527.A	590.4	154.0	03.5	
	R <sub>2</sub> '	0.0	00 0.1	70 - 00			0 0 0 0	00 100.0	0.001 00	0.0001 00	0.0001.00			1.0	00 1.0	0.1	10.0	D. D. T. 0.0			0.0001 00	001100000	0.0 0.0	1.0	45		00 10:0	0.01 00	00 100.0	0.001.00		0010000	0.0	00 0.1	71. G			0.01	0.044 .0	0.001 no	0.0001 00	
		1	:	1	# Ş		100	100	1000 1000	1000	10000		<b>3</b> C	•		0 0	95				10000	0 1000	00	9	-1 -		00 10	007 00	00100			00001 00	00	00	000			00	100	0001 00	40 1000	

### F(max) f(max									•			
1000   1000	o a	æ×		ä	_	f (min)	f(est)	۲.	4.	1	2	10
1000   1000	1			0 000	1.450	361.7	4245	2007	111	0470.	.000	770.
1000   100	!	<b>&gt; c</b>	•	100 m	1000 5000	5511.7	8.22A.3		2 5	1502	10.32	005
1,000   1,00		2 6	:•	4 609	1571		1577.4	4004	ָּבְיבְיבְּיבְיבְיבְיבִיבְּיבְיבִיבְיבְיבִיבְיבְיבְיבְיבְיבְיבְיבְיבְיבְיבְיבְיבְי	11154	S RC A	929
1000000   1000000   10000000   1000000   1000000   100000   100000   100000   100000   100000   100000   1000	1		36	462 T	530	4.77		1120	1275	1047.	939	966
1,000.00			•	466.2	447.5	6.644		2474	8000	965	23.	455
1000000   1000000   100000   100000   100000   100000   100000   100000   1000000   100000   100000   100000   100000   100000   100000   1000000   100000   100000   100000   100000   100000   100000   1000000   100000   100000   100000   1000000   100000   100000   100000   100000   100000   100000   100000   100000   100000   1000	•		40	120.4	083.1	7.650	083.3	1690	1005	200	5	96
1000000 100000   100				112	108.3	6.10.	108.3	000	040	660.	306.	981.
1000000   1000000   100000   100000   100000   100000   100000   100000   1000000   100000   100000   100000   100000   100000   100000   1000000   100000   100000   100000   100000   100000   100000   1000000   100000   100000   100000   100000   1000000   100000   100000   100000   100000   100000   100000   100000   100000   1000	•			42.4	•	A 9	14.1	1001	666	966	917.	/64.
1000001   10000   10					•		7.10		441	6.85	/19	470.
1000000000000000000000000000000000000	!		> C			7.8		000	00	2.40	620.	392
1000000000000000000000000000000000000	٠,					, ,	0		0 10 0	023	,	
10   10   10   10   10   10   10   10	٠.				•			. 400		767		7
10	٠,					7 0 0 7		, NO 0	. 4	, <b>y</b>		. CO.
10	9 (	<b>3</b> .6	•				, ,				· =	, 000
10   10   10   10   10   10   10   10	9 (	2 :	7		2020		0.7/4				, ,	
110 1000 100 100 100 100 100 100 100 10	0	5	7	177	2./4	446.5	7./5		· > 0 0 0	• •	•	-
10 1000 10.00	07	200	•	760,4	448,5	233.3	448.0	1649.	30%	000	, ,	
10 10000 10.00	10	000	•	175.9	144.8	123.9	144.9	0005	995.	.8/%	**	406.
10 100000 10.0	10	000	0.0	21.1	2,5	6.14	42.5	307.	0	.66	-	99
10   10   10   10   10   10   10   10	0	0000	0	52.1	4.2	4.1	34.2	466	942.	563.	-	781.
10   10   10   10   10   10   10   10		0000		50.0	7.7	5.0	7.7	0.00	. 466	9		φ.
10 100000 1000, 0 1 1 1 1 1 1 1 1 1 1 1	? =			18.0				. 90	442	6.45	_	470.
10 1000000 1000 1000 1000 1000 1000 10	•					` -		70	000	96.4		
100 1000 100 100 100 100 100 100 100 10	• •			· ·					0.50			
100 100 100 100 100 100 100 100 100 100	3 5					~		¥ 5 0	2.40	761.		7
100 101 100 0 11 100 0 100 100 100 100				2434.3				1000	000	379		
100 100 0.1. 1337.0 450.0 450.0 1000.0 490.0 1000.0 490.0 1000.0 1000.0 1000.0 490.0 1000.0 1000.0 1000.0 490.0 1000.0 10		) с	•	1177 7	572.4	210	572.4	000				000
100 1000 1000 1000 1000 1000 1000 1000		2 6	₹.	C C E E E	157.0	200	167.0			200		
100 1000 1000 1000 1000 1000 1000 1000	2 (	<b>3</b>	•		•				•	•	•	
100 1000 1000 1000 1000 1000 1000 1000	0	0 0	•		- ·	, ,		· (		•	•	
100 1000 1000 1000 1000 1000 1000 1000	E (	0.0	1.0			•		• • • • • • • • • • • • • • • • • • •			•	
100 100 100 100 100 100 100 100 100 100	E 1	0001	0.0	100	?:	•	?	) ) ) ()			•	
100 10000 10	C	0000	10.0	9.10	S	•		, A	546	965	• \ \ \ \ \ \ \ \ \ \ \ \ \ \ \ \ \ \ \	
100 10000 10000 10000 15.07 2.14 0.52 2.14 9961.2 9442.1 7645.8 4/19.7 14.7 14.7 14.7 14.0 16.0 16.0 16.0 16.0 16.0 16.0 16.0 16	C	10000	0.00	20.0	* •	~		000		979	•	TO!
100 10000 1000 1000 1000 1000 1000 100	0	00000	100.0	s.	~	~	~	961.	442.	4d5.	•	470.
100 1000000 10000	0	000000	0.000	٣.	6	~	٠.	50.	93.	963.	4	39%
10 10000011000110001100011 100000 100011 1000011 1000001 100001 100000 0 99999999	0	000000	0.000		٠.	•	٠.	633.	950.	923.	7.5	• 0 % •
100 100 100 100 100 100 100 100 100 100	C	0000000	0.000	3.0		•	`	994.	943.	767.	:	47.
100 100 100 100 100 100 100 100 100 100	5	100	0.0	5475.A	9.5		58.9	0000	0000	0000	. 444	.666
1000 1000 0.1. 1.0. 1.0. 1.0. 1.0. 1.0.	5	10	7	6.187.2	7.2		97.2	1909.	1000	000	000	000
000 1000 1000 1000 0 0 0 0 0 0 0 0 0 0	. 6	100		1434.7	9.7	9.4	49.7	0000	999.	.666	, 16	407
\$6000 \$6000 \$7.00 \$99.0	5	0		224.4	4.8	2.2	44.8	1000.	000	000	. 7.	. B
000 1000 1000 1000 1000 1000 1000 1000	5	000		922. A	4.4	2.5	14.4	056	966	980.	-	467.
000 10	6	000	0	24.9	4.2		4.2	000	999.	999.	41.	766.
000 100000 100.00 150.00 0.77 0.52 0.77 100.0 0.99.4 996.1 917.6 /6000 100000 100.00 10.00 0.53 0.53 0.53 0.55 9442.1 7545.4 2719.7 147 0.00 100000 10000 100.00 0.12 9531.9 6950.4 957.2 49	5	0000		52.7	3.4	~	4.5	946	945.	563.		981.
000 100000 10000 10000 10000 1000 1000	5			50,0		~	`	6.00	666	966	1/.	/ 6 A
000 1000000 10000 0 1 1 25 0 1 1 25 0 1 1 25 0 1 1 2 0 1 1 2 0 1 1 2 0 1 1 1 2 1 1 1 1					•	٠,	•	100	777	,	2	70.
\$2.750 \$1000 \$1000 \$1000 \$110 \$110 \$110 \$110					ף •	٠.		ָ ֓֞֝֞֝֞֝֝֓֞֝֝֓֓֞֝֝֓֡֓֞֝֝֓֡֓֡֓֡֓֡֓֡֓֡֓֡֓֡֓	200	· ~		0
AT STANK AND GROCKE ATTENDED TO COLD STANK AND STANK MODERN DOOR DOOR			D		•	•	•		0 4 0			
	100	K900000		•	•	•	•		, ,	?		=

columns show the effect of using the wrong frequency, as the  $R_{\rm S}$  needed to balance the bridge is given. The  $R_{\rm S}$  for resistive balance is always 1 kohm or 10 kohm. Therefore, it is evident that in some cases, the frequency must be adjusted with reasonable care.

Thus, it can be seen that a phase-angle voltmeter can be used as a null detector in a conductance bridge network with the only capacitance balancing being a rough frequency adjustment. This adjustment can be estimated very easily from Equation 30 if one knows the cell capacitances. It should be mentioned that the rapid phase-shift method of Walisch and Barthel (41) exhibits the same frequency dependence as the phase-angle voltmeter method. When Equation 21 is solved for  $\theta$  and the derivative of  $\theta$  with respect to  $R_{\rm S}$  is maximized, one finds that the  $R_{\rm S}$  necessary for balance is very close to that needed for balance when using a phase-angle voltmeter. The reason for this is that the maximum  $d\theta/dR_{\rm S}$  usually occurs near  $90^{\rm O}$ . Using the same experimental parameters as are used in Table 5, the maximum  $d\theta/dR_{\rm S}$  is always within  $3^{\rm O}$  of  $90^{\rm O}$ , and is usually within  $0.01^{\rm O}$  of  $90^{\rm O}$ .

# D. Applicability of Traditional Techniques

The phase-sensitive techniques, while considerably faster than other a-c methods, are still relatively slow (several seconds per measurement). Even self-balancing bridges cannot be used with time scales much faster than one second. The semi-balanced bridge techniques which are used to make fast conductance measurements (47 - 57) rest on

shaky theoretical ground. When the bridge is not balanced, the off-balance signal is a function of  $C_p$  and  $C_x$  as well as  $R_x$ . Furthermore, when the ionic strength of the solution changes, both  $C_p$  and  $C_x$  will change (as will  $R_x$ ), so that meaningful measurements from an unbalanced bridge are, at best, only rough approximations.

With the exception of the very time-consuming technique of Wershaw and Goldberg (34), all of the a-c techniques ignore or disregard either  $\mathbf{C}_p$  or  $\mathbf{C}_x$ . This greatly limits the experimental parameters. For example, if  $\mathbf{C}_x$  is not considered, one must be certain that  $\mathbf{C}_x$  is very large (platinization is necessary) and that the frequency is high. The use of high frequency makes the balancing of  $\mathbf{C}_p$  very difficult. If  $\mathbf{C}_p$  is not considered, the frequency must be low. This means that  $\mathbf{R}_x$  and  $\mathbf{C}_x$  must be very large because of  $\mathbf{Z}_F$ . Therefore, a compromise frequency is normally used. The magnitude of this frequency depends on the experimental parameters, as has been shown for the Kohlrausch and phasedetector bridges.

The four-electrode d-c technique solves the capacitance problems but cannot be used to follow fast conductance changes because of the cell design (a possible exception to this might be to follow fast changes after a P-jump). The d-c technique also has several experimental difficulties, such as the requirement of reversible point-electrodes. Both the d-c and a-c techniques cause considerable solution heating because the signals are applied continuously.

Thus, the traditional techniques for conductance measurements can be used accurately if, and only if, one carefully considers the accuracy required, the cell capacitances and resistance, the frequency (including d-c) and magnitude of the signal source, the null detector characteristics, and the power dissipation in the cell. The apparatus, cell, and experiment must then be designed for these parameters.

	•		
<b>r</b> '			
5			
<b>©</b> rig			

j

#### IV. THE BIPOLAR PULSE TECHNIQUE

#### A. Theory

The bipolar pulse technique involves the application of two successive constant voltage pulses of equal magnitude but opposite polarity to the conductance cell, and the measurement of the current passing through the cell at the end of the second pulse. Since the pulses can be as short as 20 µsec, the effect on  $C_d$  and  $Z_F$  is the same as when a very high frequency is used, since  $\mathbf{C}_{\mathbf{d}}$  is only slightly polarized. Assuming the lead and contact resistance can be reduced to a vanishingly small value, C, and C; (because of small polarization) will experience the same potential. Assuming the pulse width is much greater than  $R_tC_t$ ,  $C_t$  may be considered in parallel with  $C_i$  and  $C_c$ , giving a total parallel capacitance of  $C_p$ . Thus, ignoring only  $R_c$ , the cell can be accurately represented by the simplified equivalent circuit shown in Figure 4 when using the bipolar pulse technique. The sequence of events in the measurement is described qualitatively below.

At the beginning of the first pulse,  $C_p$  will charge quickly causing a spike in the cell current. If  $t_1 << R_x C_x$ , the voltage  $(e_c)$  developed across  $C_x$  will be small and increase approximately linearly with time. Thus, the current flowing through  $R_x$  and  $C_x$  will drop slightly during  $t_1$  due to the charging of  $C_x$ . When the polarity is reversed at the start



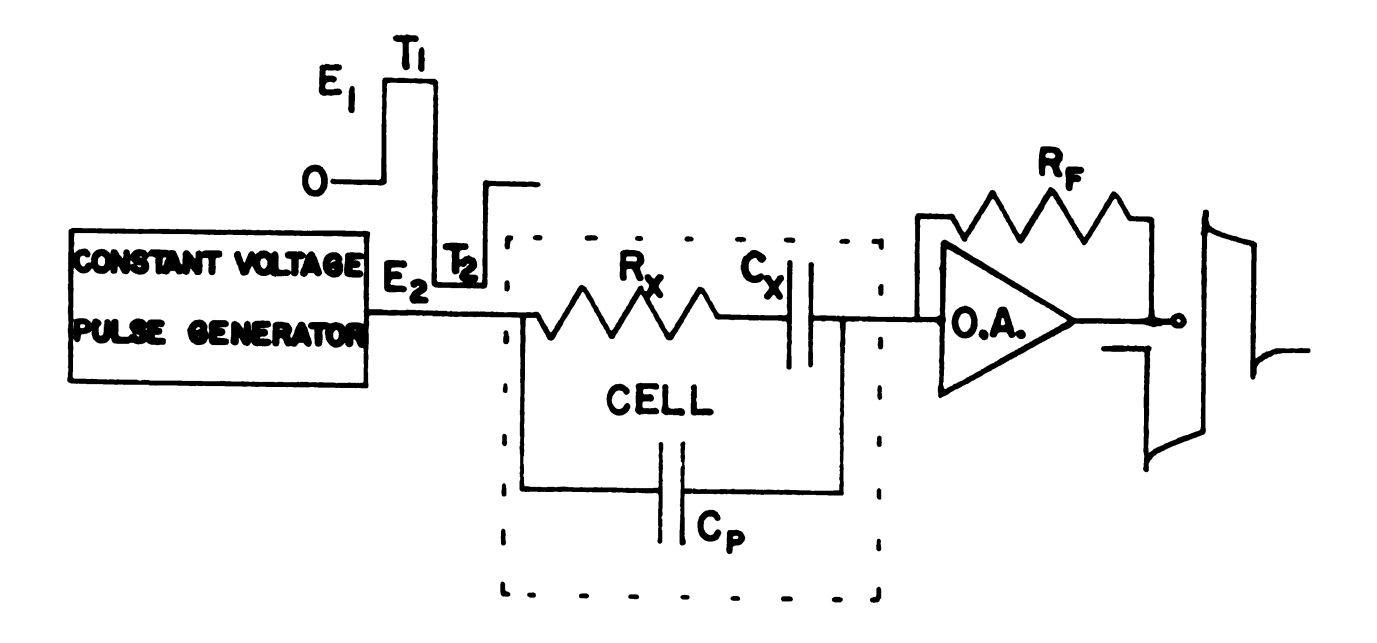


Figure 4

A Bipolar Pulse Conductance Device

of  $t_2$ ,  $C_p$  will again charge quickly to the new potential. The current through  $R_x$  and  $C_x$  will be enhanced because of the potential,  $e_c$ , accumulated during  $t_1$ . However, during  $t_2$ ,  $C_x$  will discharge the same number of coulombs that it charged during  $t_1$ . This causes a decrease in current until, at the end of  $t_2$ , the entire voltage drop across the cell is due to the voltage drop across  $R_x$  (since  $C_x$  is completely discharged). At the end of  $t_2$ ,  $e_c = 0$  and no current is flowing through  $C_p$  since it is at constant potential. Therefore, the instantaneous current through the cell at the end of  $t_2$  is simply  $i = e_2/R_x$ . Thus, the instantaneous current measured at this time is directly proportional to the conductance and independent of  $C_x$  and  $C_p$ .

ca

## B. Theoretical Error Analysis

At this point, it is fruitful to examine the circuit and measurement sequence more closely to get an idea of the theoretical error limits and the instrumental tolerances required. At the end of  $t_1$ ,

$$(e_c)_1 = e_1[1 - \exp(-t_1/R_xC_x)]$$
 (1)

and at the end of  $t_2$ ,

$$(e_c)_2 = e_2 \left[ 1 - exp \frac{-t_2}{R_x C_x} \right] + e_1 exp \frac{-t_2}{R_x C_x} \left[ 1 - exp \frac{-t_1}{R_x C_x} \right]$$
 (2)

Since the measured conductance is

$$G = \left[e_2 - \left(e_0\right)_2\right] / R_x \tag{3}$$

and the conductance should be

$$G_{o} = e_{2}/R_{x} \tag{4}$$

the relative error due to polarization is

$$Q = (G - G_0)/G_0 = -(e_c)_2/e_2$$
 (5)

A series expansion of the exponentials in Equation 2 gives the following expression for Q in terms of dimensionless parameters:

$$Q = b(a - 1) - \frac{b^2[a(d + 2) - 1]}{2} + \frac{b^3[a(d^2 + 3d + 3) - 1]}{6} - \dots$$
(6)

where  $a = -e_1 t_1/e_2 t_2 \approx 1$  (a = 1 for truly complementary pulses)

$$b = t_2/R_xC_x$$

and  $d = t_1/t_2 = 1$ 

If a = 1 and d = 1, then  $Q = -b^2$ . Even for the unfavorable case of  $R_X = 200 \ \Omega$ ,  $C_X = 10 \ \mu\text{F}$ , and  $t_2 = 20 \ \mu\text{sec}$ ,  $Q = -10^{-4}$ 

or -0.01%. If, in this example, there is a 1% deviation from having complementary pulses, i.e.,  $a = 1 \pm 0.01$ ,

$$Q \approx 10^{-2}(\frac{1}{2}0.01) - 10^{-4}[3(1\frac{1}{2}0.01) - 1]/2$$

or 
$$Q = -1.5 \times 10^{-6}$$
 if  $a = 1.01$ 

and 
$$Q = -1.99 \times 10^{-l_{\downarrow}}$$
 if  $a = 0.99$ 

If, in addition,  $t_1$  and  $t_2$  differ by 10%, <u>i.e.</u>,  $d = 1 \pm 0.1$ ,  $Q_{max} \simeq -10^{-4} - 10^{-4} [3.1 \times 0.99 - 1]/2 \simeq -2.03 \times 10^{-4}$ If  $C_x$  or  $R_x$  is increased, the resulting error is cut accordingly. For example, if  $R_x = 2 \text{ k}\Omega$ ,

$$Q_{\text{max}} \simeq -10^{-5} - 10^{-6} \times 1.03 \simeq -1.1 \times 10^{-5}$$

Theoretically, there is no dependence on  $C_p$  (as long as  $C_pR_o < 5$  t<sub>2</sub>, where  $R_o$  is the output impedance of the pulse generator) since at the end of the pulse,  $C_p$  has already charged to the constant voltage. Also, there is no theoretical limit on  $R_x$  if  $C_x$  and t<sub>2</sub> have appropriate values. Thus, if one can apply a complementary pulse pair matched to within 1%, and keep the time short enough so that the maximum double layer voltage,  $(e_c)_1$ , is less than 1% of the applied voltage, a measurement of the current at the end of the second pulse will give the conductance to within 0.02%, regardless of  $C_p$  and  $C_x$ .

# C. The Instrument

With these requirements in mind, the bipolar pulse conductance device shown in Figure 5 was designed.

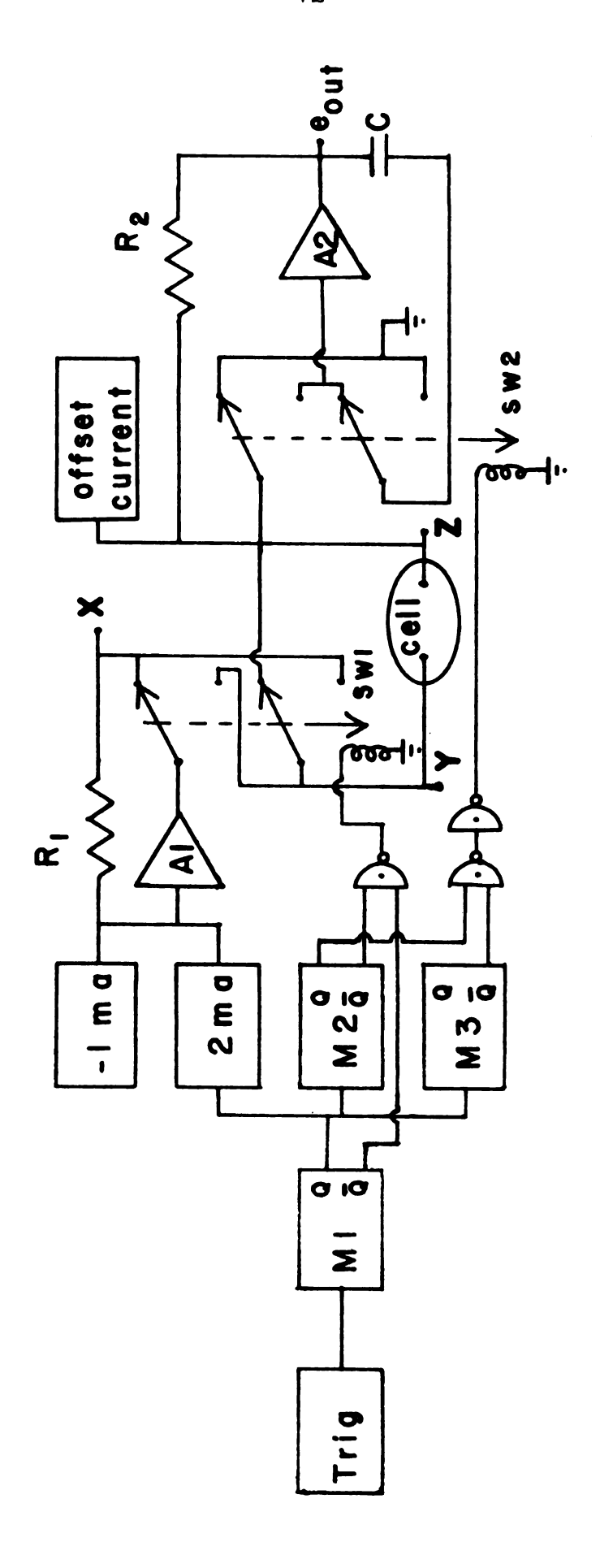
The time sequence of events is shown in Figure 6, with the important times labeled A, B, C, and D. Figures 5 and 6 may be used with the following explanation to understand the

The Prototype Bipolar Pulse Instrument

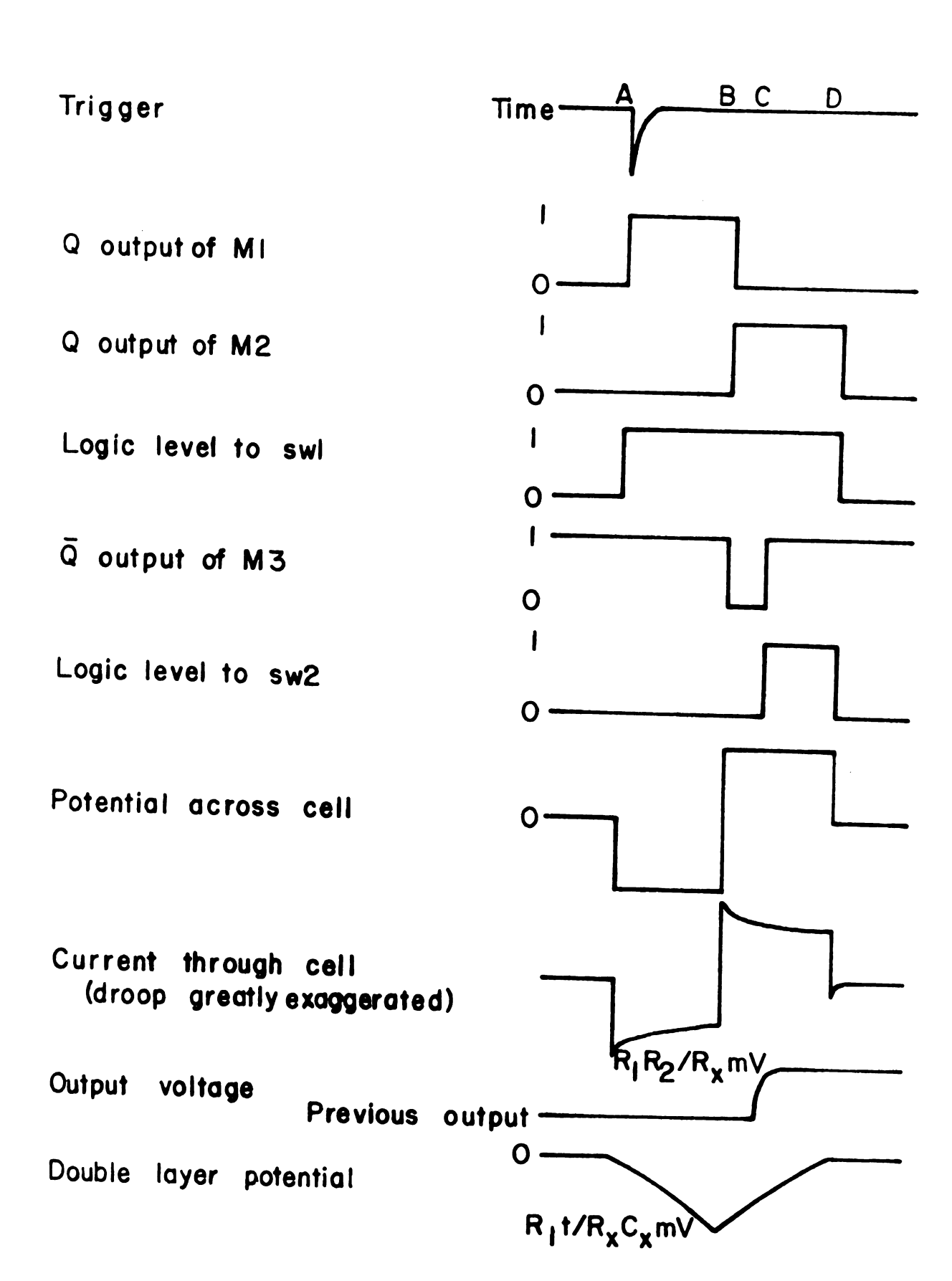
 $R_1 = 10 \text{ turn}$ ,  $10 \text{ k}\Omega \text{ pot}$ 

 $R_2 = 10, 100, or 1000 k\Omega$ 

Switches are dual drain, enhancement-mode MOS-FET transistors.



Timing Sequence During Measurement



-1				

instrument functions during the measurement sequence.

Time A. The trigger source can be the internal unijunction oscillator, line frequency via the unijunction transistor, or some external trigger source. The repetition rate can be varied between 0.5 - 20,000 Hz, depending on the particular needs of the experiment. In any case, the trigger logic produces a negative-going pulse, which triggers monostable 1. M1 turns "on" the +2 mA going to A1, changing the voltage at point X from +R<sub>1</sub>mV/ $\Omega$  to -R<sub>1</sub>mV/ $\Omega$ . M1 also causes sw1 to go "on" so that points X and Y are connected together. Point Z remains at ground (through sw2). A large instantaneous current flows as  $C_p$  is charged as fast as amplifier A1 can provide current. A voltage begins to develop across  $C_X$  as time progresses. The output voltage  $e_0$  is not yet affected.

Time B. M1 goes "off" (after 20, 200, or 2,000 µsec, depending on pulse-width setting), triggering M2 and M3, and turning "off" the +2 mA going to A1 so that point X and point Y return to  $+R_1mV/\Omega$ . Sw1 and sw2 remain in their previous states and the current that flows through  $C_p$  is again carried to ground through sw2.

Time C. M3 goes "off", turning sw2 "on", putting A2 in the sampling mode. Point Z is connected to virtual ground instead of ground, and A2 charges C to a new voltage, so that at time D,  $e_0 = -R_1R_2/R_x$  mV/ $\Omega$ . It should be mentioned that M3 is used for the sole purpose of ensuring that  $C_p$  has been fully charged before A2 begins sampling (this prevents output spikes). This is especially necessary

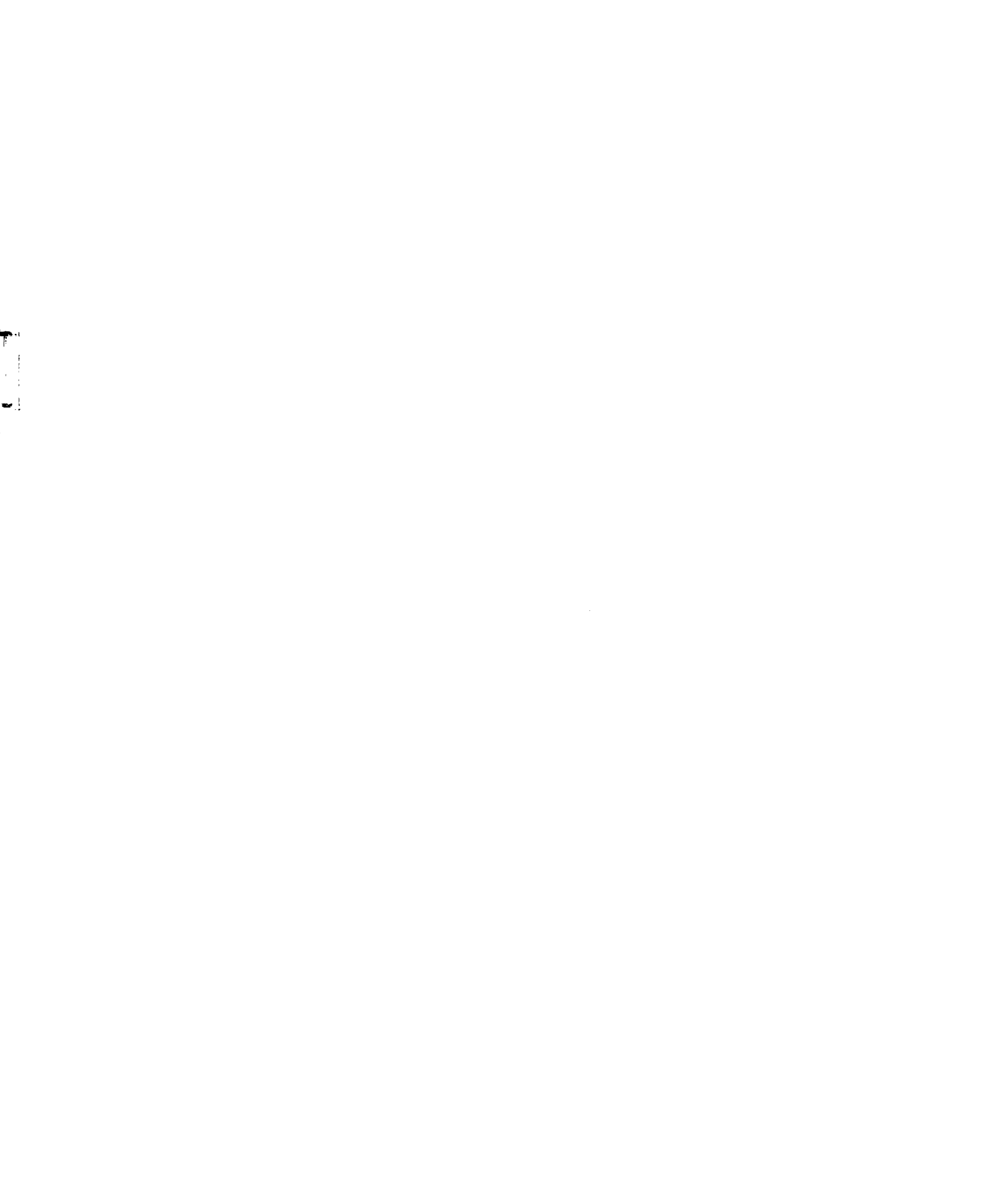
when both C<sub>p</sub> and R<sub>2</sub> are large.

Time D. M2 goes "off", disconnecting point X from point Y as sw1 goes "off". Also, the cell leads are shorted together to equalize any slight polarization developed by the end of the second pulse. Sw2 also goes "off", putting A2 in the holding mode. The output remains proportional to the current passing through the cell at the end of the second pulse (which has been shown to be  $e_2/R_x$ ). Point Z is again connected to ground so that both sides of the conductance cell are at ground potential. This condition remains until the next trigger pulse starts another cycle.

It is important to realize that the current going through the cell in no way affects the constant potential of the pulses, despite the resistance of sw1. This resistance does affect the potential, but this potential is not a function of the cell current. Then sw1 is "on", the feedback resistance of Al is  $R_1^* + R_{sw}$  ( $R_1^*$  is a 10 turn, 10 kohm pot), as shown in Figure 7, and point Y becomes the controlled point.

It is also important to note that during the sampling of the current, the switch resistances do not affect the accuracy since point Z is controlled to be at virtual ground. In the prototype instrument, there is a possibility of introducing error due to the resistance of sw2 in the hold mode when sw1 is "on". The resistance of sw2 can essentially make the pulses non-complementary, i.e.:

$$a = \frac{-(e_1 - R_{sw} i_{cell})t_1}{e_2 t_2} \approx 1 + \frac{R_{sw}}{R_v} \quad \text{if} \quad \frac{e_1 t_1}{e_2 t_2} = -1$$



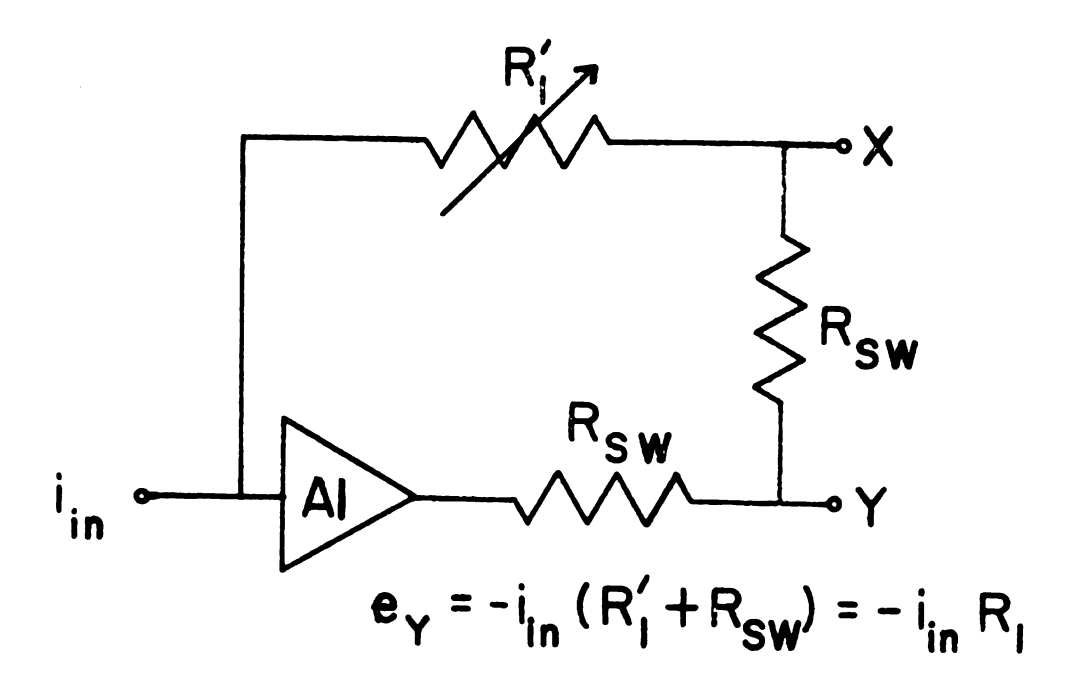


Figure 7
Constant Potential Generator

Thus, if "a" is important, as would be the case for large  $t/R_{\rm X}C_{\rm X}$ , this could introduce error. Notice that both  $R_{\rm X}$  and  $C_{\rm X}$  must be small (or t large) before "a" becomes an important consideration (as in the use of small, unplatinized electrodes).

As might be expected, the switches were a design problem since they were required to have very low "on" resistance, very high "off" resistance, carry both polarity signals, and be very fast. P-channel, enhancement-mode MOS-FETs fulfill these criteria quite well when used with an appropriate driving circuit. The "on" resistance is less than 50 ohm, and the "off" resistance is essentially infinite. There is a leakage current from the gate of approximately 10<sup>-10</sup> amps. This causes a drift of

approximately 10 mV/sec in the hold mode of the sample and hold current amplifier. The switching time is less than l µsec.

#### D. Instrumental Tests

#### 1. Linearity Test

If the output is proportional to the conductance, then,  $e_0 = K/R_X + E_{\bullet}$ , where K is some constant, and  $E_{\bullet}$  is  $e_0$  when  $R_X = -(E_{\bullet}$  can be adjusted using the offset current source). If  $E_{\bullet} = 0$ , then  $K = e_0 R_X$ . Figure 8 shows the product

If  $E_{\infty}=0$ , then  $K=e_0R_X$ . Figure 8 shows the product  $e_0R_X$  vs.  $e_0$ . The measurements were made using an ESI Potentiometric Voltage Bridge to measure the output voltage, and an ESI 0.01% decade resistance box for  $R_X$ . In this experiment, it is obvious that the linearity is excellent over the full output voltage range, always falling within 0.01% of full scale (10 V). This indicates that if absolute accuracy is needed, only one standardization need by made by replacing the cell with a standard resistor  $(R_S)$ . The absolute conductance is then  $1/R_X=e_X/e_SR_S$ , where  $e_X$  is  $e_0$  with  $R_S$ , and  $e_S$  is  $e_0$  with  $R_S$ .

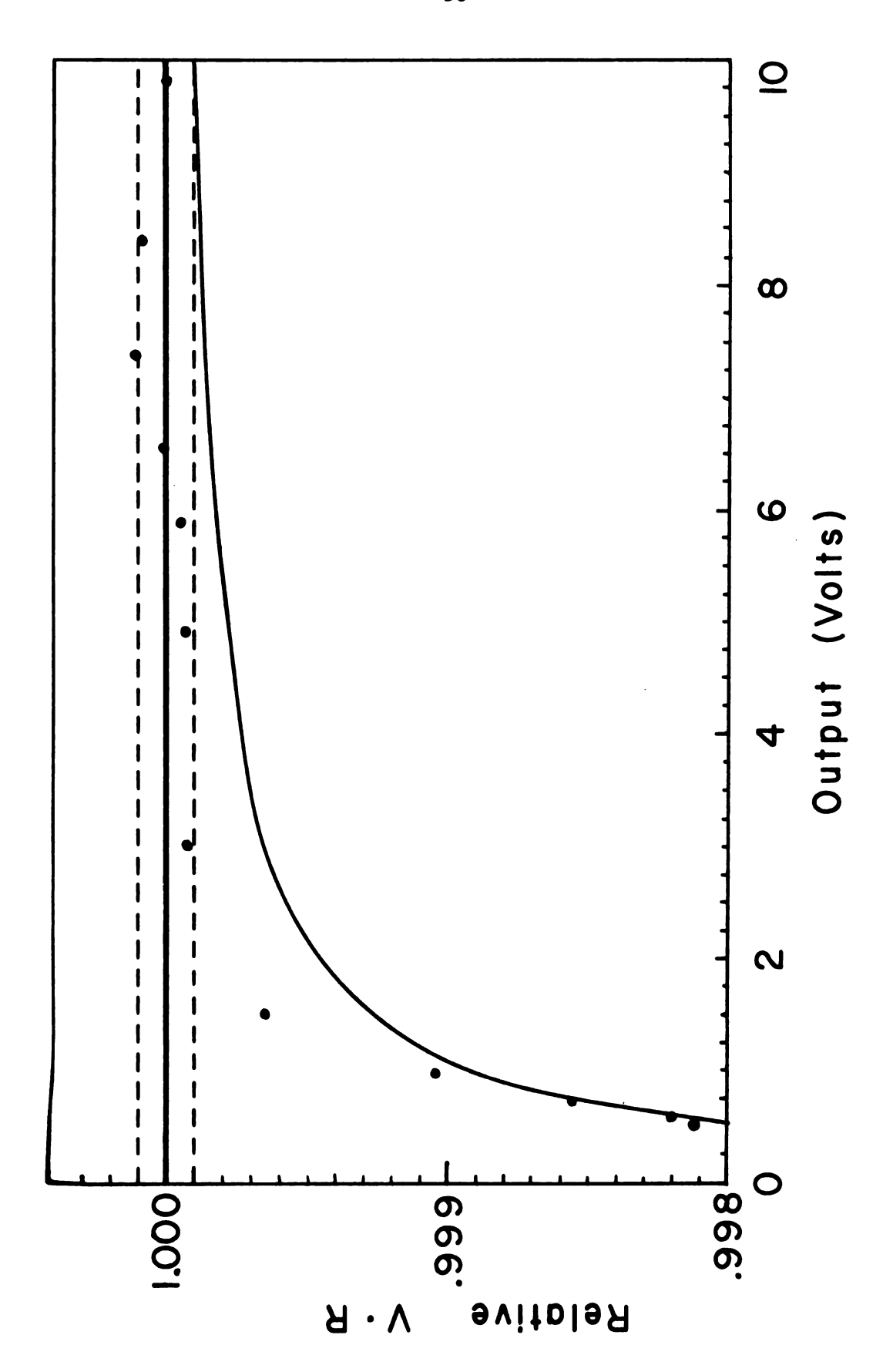
## 2. Dependence on Parallel Cell Capacitance

 $C_p$  was varied between 0 and 1000 pF for resistances between 200 ohm and 10 Mohm. There was no observable dependence (0.004%) on the magnitude of  $e_0$  for any resistance value. However, for very high resistance ( $R_X \ge 1$  Mohm), there was some scatter in the output due to the fact that the capacitor turned the operational amplifier into a high

# Linearity Test

Dashed line = 0.01% absolute deviation

Solid line = 0.01% relative deviation



gain differentiator with a 1 Mohm resistor in the feedback loop. For example, with  $R_{\rm x}=1$  Mohm and  $C_{\rm p}=1000$  pF, the relative scatter was 0.2%. This is, however, a condition which has no physical significance because  $C_{\rm p}$  would never be that high, and especially not for a 1 Mohm solution resistance.

### 3. Dependence on Series Cell Capacitance

A dummy cell consisting of a capacitor (0.05 - 10 uF) and a resistor (1 kohm - 1 Mohm) in series was made to test the dependence of the conductance measurement on the series capacitance. It should be noted that the largest capacitor (10 µF) used is still much smaller than  $\frac{1}{2}$  the typical double layer capacitance. The results of the experiment are shown in Table 6.

From Table 6, it is obvious that there is a trend toward larger errors as  $R_{\chi}$  and  $C_{\chi}$  decrease and as t increases (a completely expected result). For large resistances, the pulse length is increased to allow the amplifier (A2) to reach its final voltage before making a measurement. For the low conductance ranges, the feedback resistor (R2) is either 100 kohm or 1 Mohm, and 20 usec may not be enough time to achieve the final voltage. It should be noted that in these conductance ranges, very little current flows through the cell, so  $C_{\chi}$  still does not charge significantly. If one uses a typical conductance cell in which  $C_{\chi} \ge 100~\mu\text{F}$ , the errors would all be negligible, even for lower resistances. In a situation in which unplatinized electrodes must be used (such as in some non-aqueous work), the resistance is

TABLE 6

Dependence on  $C_{\chi}$ 

R <sub>x</sub>		% ]	Error for	r C <sub>x</sub> in ;	uF	
	10	1	0.5	0.2	0.1	0.05
l ks	0.050	0.861	1.930			
5 ks	0.007	0.059	0.091	0.197	•	
10 ks	0.005	0.046	0.080	0.163	0.423	t = 20 µsec
50 ks	0.001	0.020	0.042	0.103	0.206	
100 ks	0.000	0.003	0.010	0.036	0.085	0.252
	-					
50 ks	0.006	0.024	0.042	0.137		+ 0.3 mass
100 ks	0.005	0.008	0.028	0.069		t = 0.2  msec
500 ks	0.001	0.004	0.026	0.058	0.122	0.300
1 M.	0.000	0.001	0.005	0.017	0.042	0.133

normally high so that the decrease in  $C_{\chi}$  is compensated for by an increase in  $R_{\chi}$ . Therefore, the error remains small. In any case, the error involved using this technique is smaller than the error involved when using a bridge technique on the same system.

# 4. A-C Bridge Comparison

The conductance of three solutions was measured using both this instrument and a modified Wien bridge (65). Below 10 kohm the two methods agreed to better than 0.1%, but at 60 kohm, the bridge could not be nulled and was about 2% high.

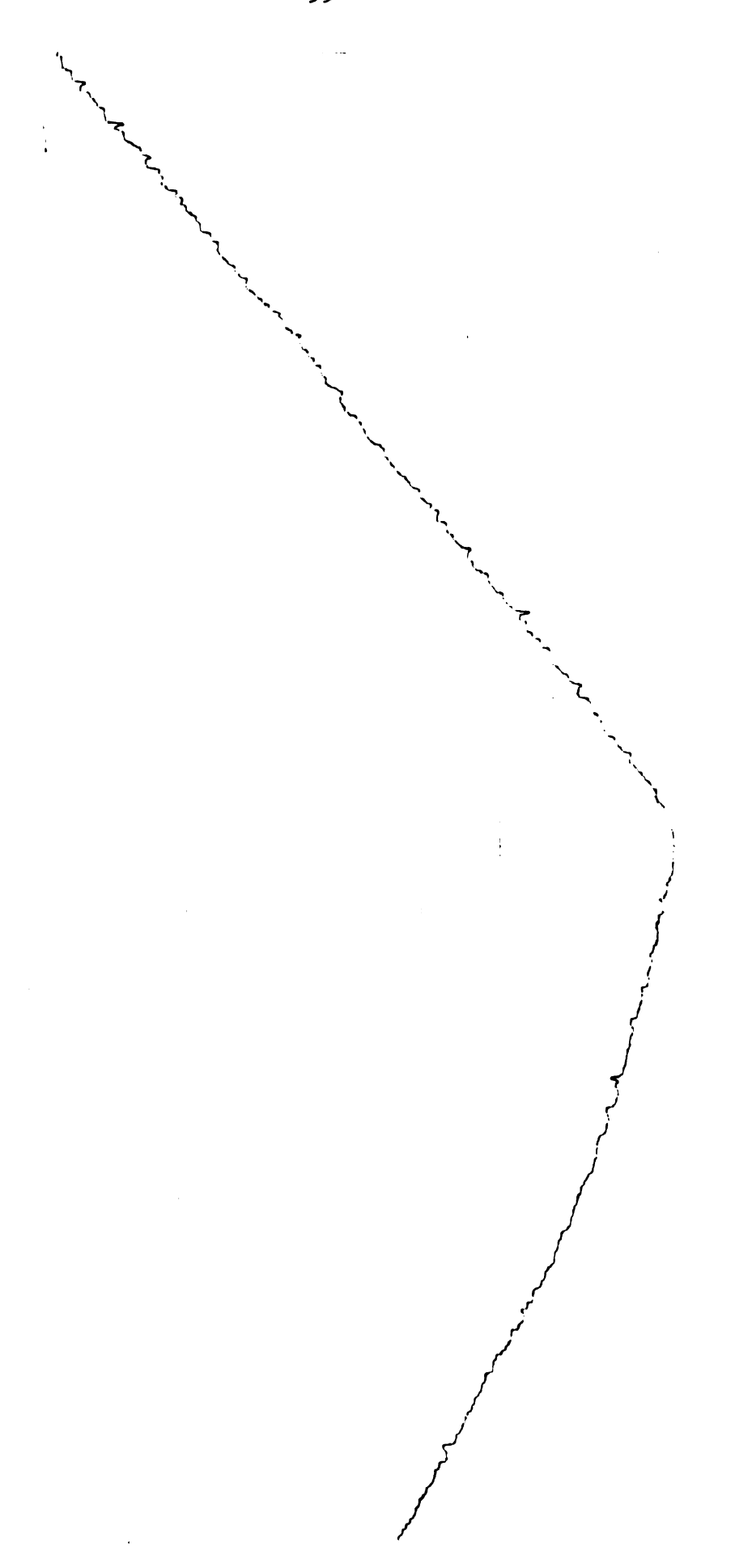
# E. Instrument Tests on Chemical Systems

## 1. Acid - Base Titration

As a first test, the chemically uninteresting reaction between an acid and base was followed conductometrically. A solution that was 10<sup>-3</sup> M in HCl was titrated with 5 M NaOH using a constant delivery burrette. Delivery was made through a capillary tube with a 15-foot hydrostatic head to provide constant pressure. A typical curve is shown in Figure 9. The experiment was repeated several times, and in each case, the same shaped curve was obtained. When the amount of HCl was varied, the endpoint was proportional to concentration, but the magnitude of the minimum remained unchanged. From this minimum, one can calculate the ratio of the equivalent conductances of NaCl to HCl of 0.296. This compares very favorably with the Kohlrausch ratio of 0.297.

Acid - Base Titration

0.001 M HCl with 5 M NaOH



## 2. Reaction Rate Studies

The pseudo first-order reaction between ethanol and acetyl chloride was studied at three different temperatures. The ethanol was dried by the method of Lund and Bjerrum (66), and the acetyl chloride was used without further purification. Approximately 3 µl of acetyl chloride was injected into 125 ml of ethanol for each experiment. Several experiments were run in the same solution (using the current offset to keep the same sensitivity), and no significant deviation was found between runs. The conductance change was measured using a Heath Universal Digital Instrument (UDI) in the digital voltmeter mode (0.1 sec aperture), with a period of 1.500 sec between measurements. Every fourth measurement was manually recorded (with another UDI keeping track of counts) so that a data point was obtained every six seconds. The rate constants were obtained using the three parameter least squares curve-fit computer program, which is included in the appendix. This program was written for the PDP 8/i computer, but could easily be revised to adapt to other systems. It minimizes the general equation:

$$E = \sum_{i=1}^{n} \left[ Y_i + B \cdot \exp(-kX_i) - A \right]^2$$
 (7)

where  $X_i$  and  $Y_i$  are the data points, and A, B, and k are the curve-fit constants (k = rate constant). To guarantee convergence, a modification of the Gauss - Newton successive approximation method was used. It is similar to the modification by Hartley (67), which Daum (68) used in his treatment of current impulse data. The results are given in Table 7.

TABLE 7

Reaction Rate Studies -- Acetyl Chloride and Ethanol

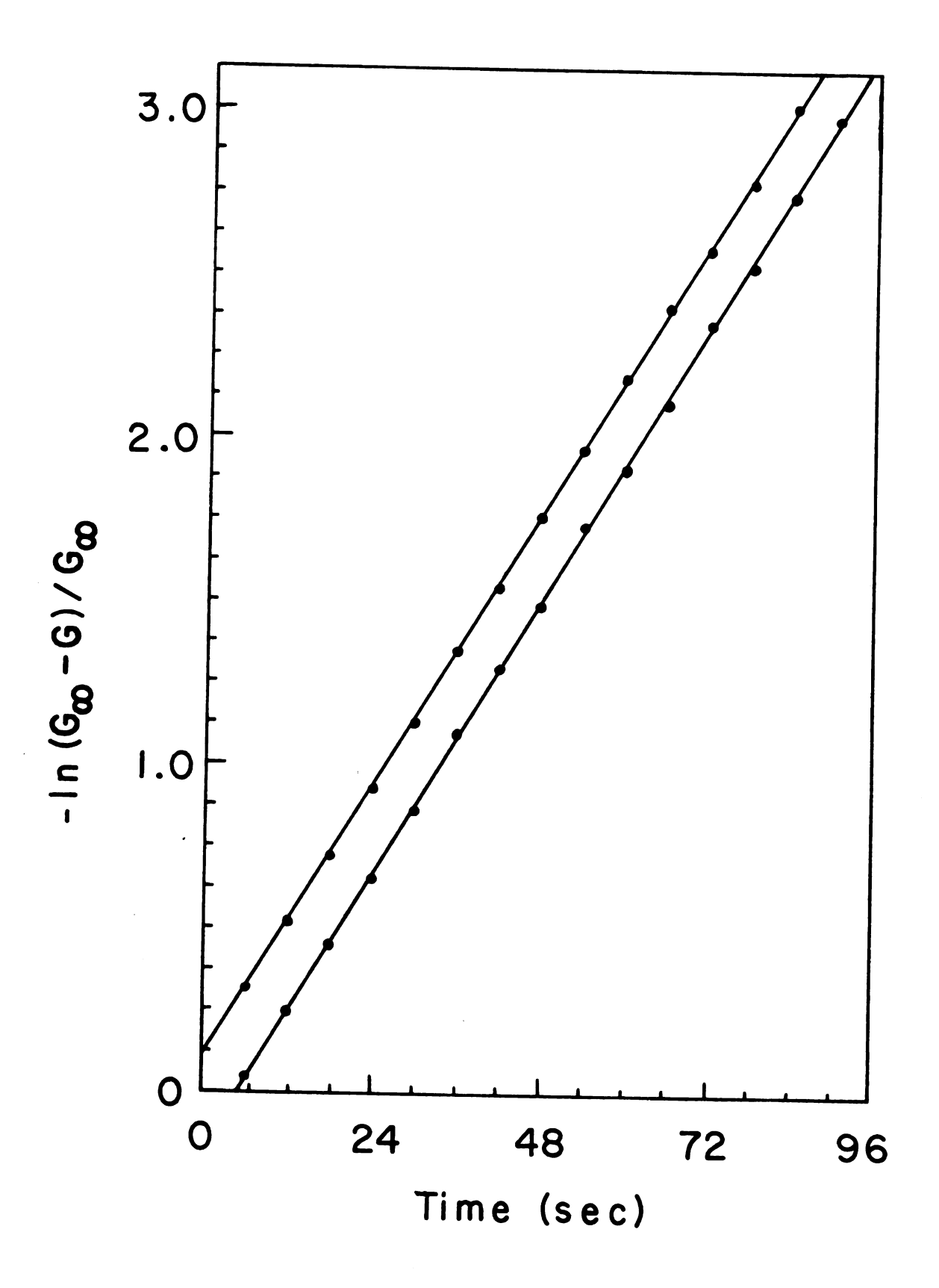
Temperature	k (sec <sup>-1</sup> ) $\pm$ std. dev.	Number of Runs
4.74°C	0.0306±0.0002	7
6.40°C	0.0346±0.0002	5
15.01°C	0.0700±0.0007	15

Typical plots of  $\ell n$  (G<sub>o</sub> - G)/G<sub>o</sub> vs. time are shown in Figure 10. The standard scatter for a typical experiment is less than 0.1%. The data obtained agree very well with data obtained by Euranto and Leimu (50), who used a rather complicated, fast-quenching titrametric method. Their data and these data obtained conductometrically are shown in the Arrhenius plot in Figure 11.

assumed during the reactions, although this is not strictly true. The temperature of the bath was constant, but the heat of reaction, and to some extent, the original higher temperature of the acetyl chloride, caused the temperature to increase by about 0.01°C during the reaction. A temperature profile is shown in Figure 12 for a 5 - 6 times greater concentration of acetyl chloride than was used to determine the reaction rate. These data were obtained by using the bipolar pulse conductance instrument to measure the conductance of a calibrated thermistor in place of the conductance cell. This instrument permits a rapid, accurate measurement

Reaction Rate Studies

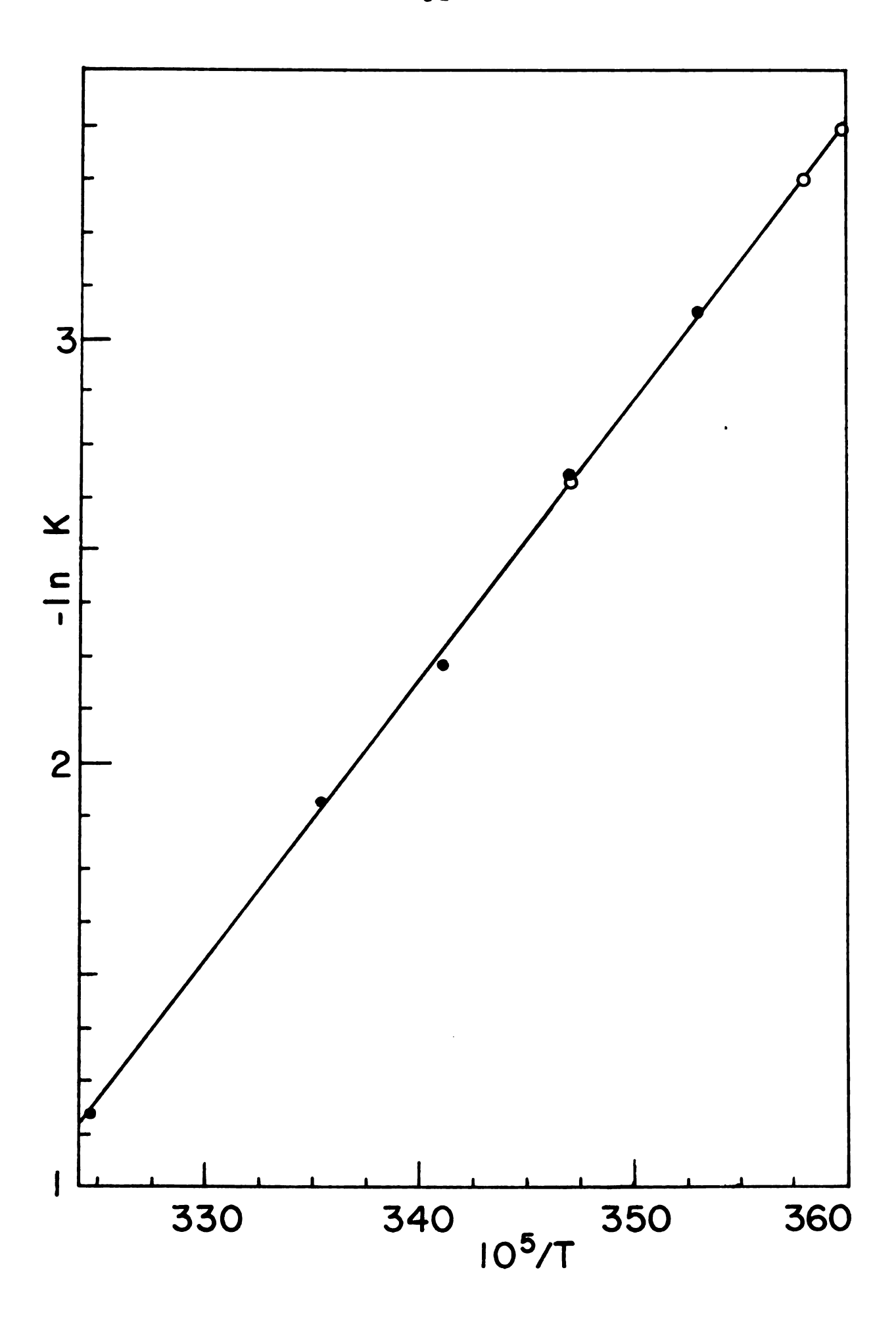
Acetyl chloride (3  $\mu$ l) and ethanol (125 ml) Consecutive reactions at 6.40  $^{\circ}$ C



Temperature Dependence of Reaction Rate

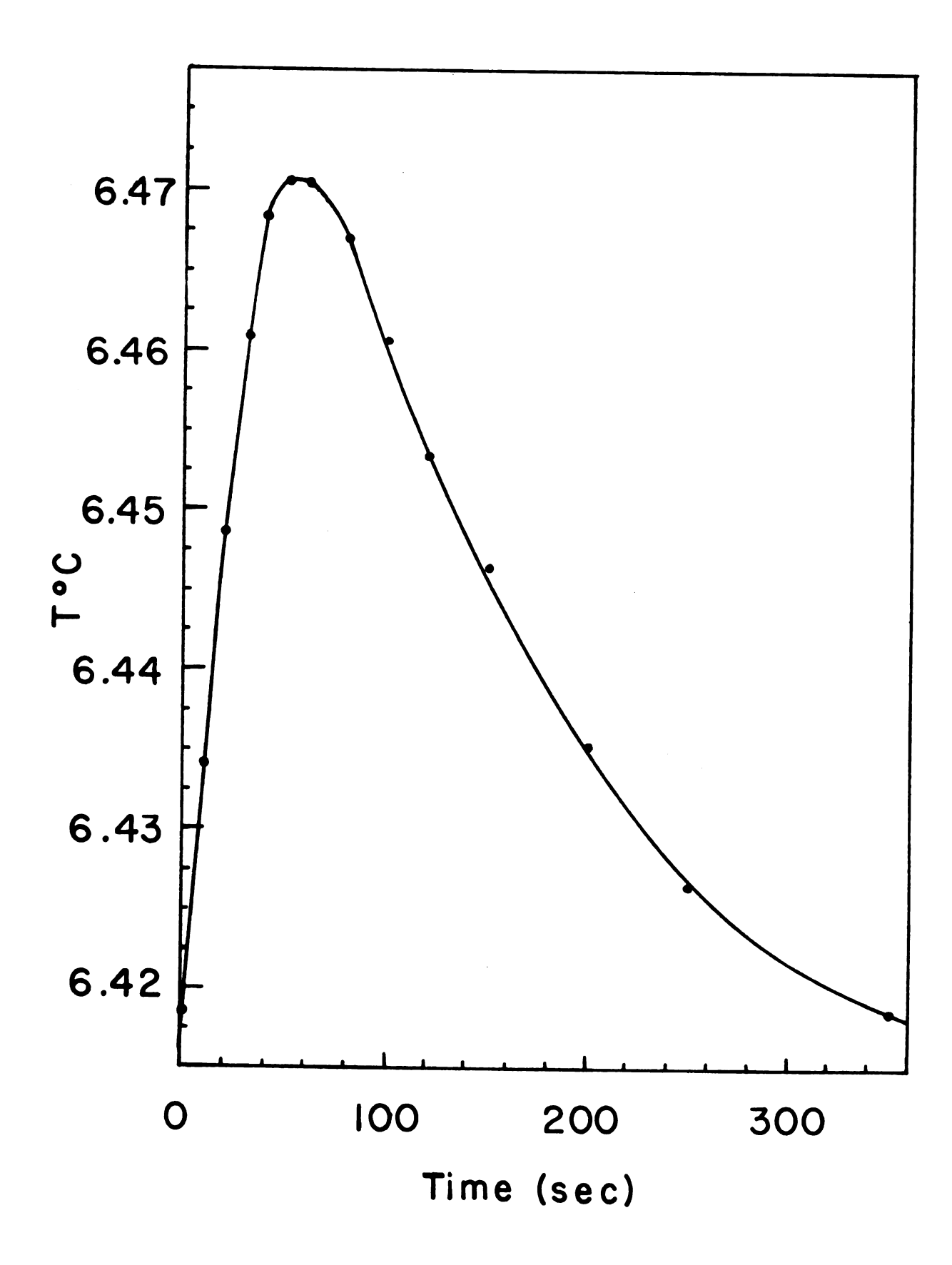
Circles obtained conductometrically

Dots obtained by another method



Temperature Profile During Reaction

18  $\mu$ l acetyl chloride into 125 ml ethanol at 6.42°C



of temperature with extremely little solution heating.

The half-lives of these reactions were between 10 - 20 seconds. Much faster reactions could be studied if appropriate readout and recording were used. Reactions with half-lives of less than 1 msec could easily be followed using stopped-flow or other techniques. Since the output is proportional to concentration, the results are very easy to manipulate.

### 3. Conductometric EDTA Titration of Zinc

Known volumes of 0.04 M  $Zn(NO_3)_2$  and pH 10 buffer (0.55 M NH<sub>3</sub> and 0.10 M NH<sub>h</sub>Cl) were pipetted into a beaker and diluted to 125 ml. The resulting solution was titrated with a 0.1007 M EDTA solution using a Sargent Automatic Burrette (10 ml). The conductance cell consisted of two unplatinized platinum disks 1 cm in diameter and 1 cm apart. The solution resistance varied between 21 and 35 ohm, depending on initial concentrations of zinc and buffer, and the change at the endpoint was only about 0.02 ohm (0.1% of total). This is truly a worst case situation since the conductance instrument was not designed to operate below The noise level was under 0.01% of the total con-200 ohm! ductance, even at this very high conductivity. The change in conductance was recorded on a strip chart recorder at 5 in/min with a full-scale sensitivity of 175 µmhos (about 0.5% of the total conductance). The offset current source was used to "buck out" about 99.5% of the total cell current.

Typical endpoints are shown in Figure 13 for 10 ml of the zinc solution and varying amounts of buffer. Notice that

### Figure 13

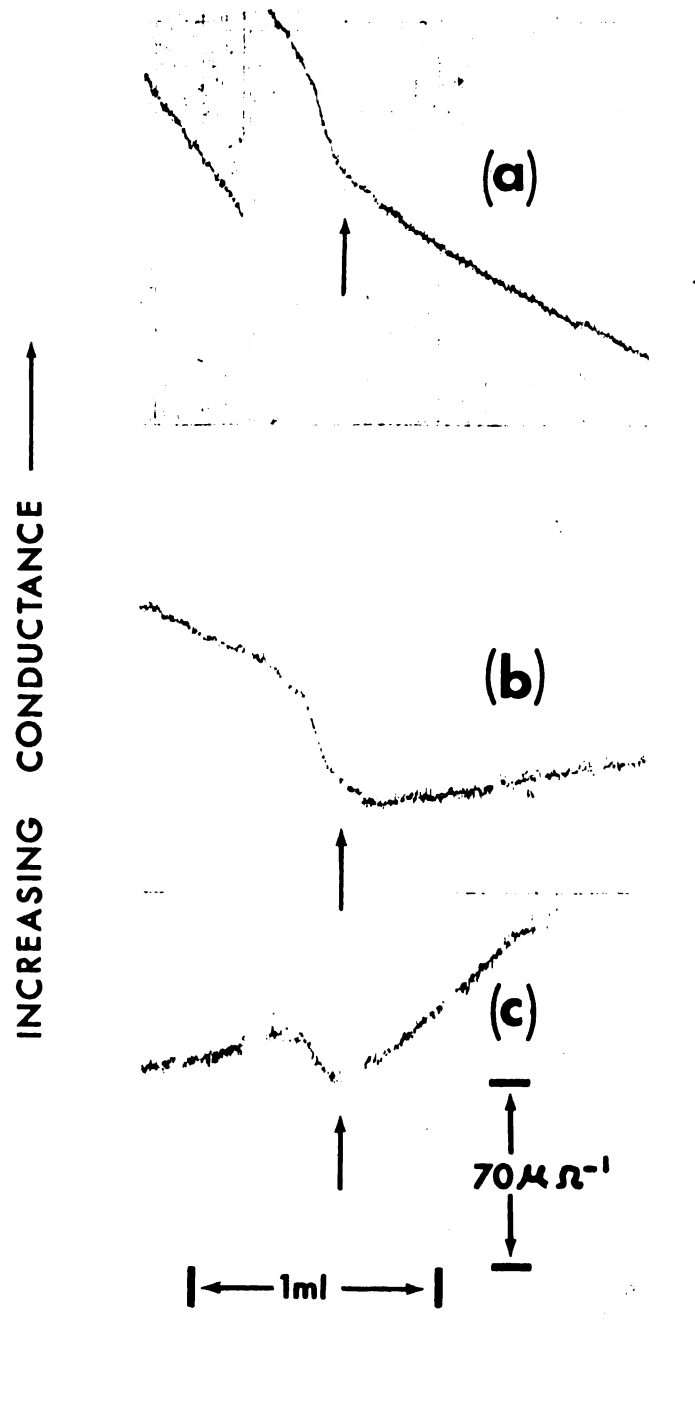
Conductometric EDTA Titration of Zinc

- (a) 10 ml buffer (0.0281  $\Omega^{-1}$ )
- (b) 15 ml buffer  $(0.0377 \Omega^{-1})$
- (c) 20 ml buffer  $(0.0476 \Omega^{-1})$

Full scale = 175  $\mu\Omega^{-1}$ 

Arrows indicate endpoint

Sharp breaks due to changing the offset current



- INCREASING VOLUME

this is not a "typical" conductance titration curve in that there are actually two breaks near the endpoint. The first break is taken as the endpoint for the following reasons:

- (1) The first break is proportional to the amount of zinc added (whereas the second break is not.)
- (2) There is a sharp conductance increase which levels off to a more moderate increase even when no zinc solution is added (only 15 ml of pH 10 buffer).
- (3) The first break agrees within 0.2% with an Eriochrome Black T titration on the same system.

While it is not the purpose of this thesis to enter into a detailed study of equilibria, a few observations of the behavior near the endpoint should be mentioned. The pH is constant to within 0.001 pH unit throughout the titration, as recorded using a Heath expanded scale pH meter/recorder. It is not a slow, rate-controlled process, but rather an equilibrium situation. The same type of endpoint behavior is obtained when calcium is used instead of zinc. The difference between the initial and intermediate (between breaks 1 and 2) slopes is independent of both the zinc and buffer concentrations. This slope is:

3.2 $\pm$ 0.2 ver div/hor div x 5 hor div/ml . x 17.5  $\mu$ mhos/ver div = 270  $\mu$ mhos/ml of EDTA.

Assume that the conductance is proportional to the total normality, then  $G = K \cdot N$  where K is a constant. Before the endpoint, the reaction is:

$$2 NH_3 + Zn^{2+} \xrightarrow{2 Na^+, H_2Y^{2-}} ZnY^{2-} + 2 NH_4^+ + 2 Na^+$$
 (8)

yielding an increase in ions of 0.4 meq/ml of EDTA. In the case of 15 ml of buffer, the conductance is practically

constant before the endpoint. Thus, the increase in ions is almost exactly offset by the dilution with titrant. Therefore, in this case.

$$N = 0.4 \text{ meg/ml}$$

and

$$K = \frac{0.0377\Omega^{-1}}{0.4 \text{ meg/m}1} = 0.1 \Omega^{-1} \text{ ml meg}^{-1}$$

After the endpoint, the reaction (at pH 10) is

$$3 \text{ NH}_{3} \xrightarrow{4 \text{ Na}^{+}, 2 \text{ H}_{2}Y^{2-}} 3 \text{ NH}_{4}^{+} + \text{HY}^{3-} + Y^{4-} + 4 \text{ Na}^{+}$$
 (9)

yielding an increase of 0.7 meq/ml of EDTA. Of this,
0.4 meq/ml is needed to offset dilution and the remaining
0.3 meq/ml increases the conductance of the entire solution.
Thus, the slope after the endpoint should be:

$$\frac{0.3 \text{ meg/ml EDTA}}{129 \text{ ml}} \times 0.1 \text{ ml } \Omega^{-1} = 230 \text{ } \mu\text{mhos/ml EDTA}$$

which is very nearly the experimental result.

These data tend to point toward the formation of a complex between EDTA and  $NH_4^+$  after the EDTA concentration is built up following the endpoint.

The endpoint is easily detectable, even though it must be continuously recorded rather than obtained by making a few measurements and drawing intersecting lines. The result of seven runs with different volumes of zinc and buffer solutions is:

$$2.132 \pm 0.003$$
 inches/ml of  $Zn^{2+}$ 

A volume reading of 6095 on the burrette was found to be equivalent to 42.31 inches of chart paper. The experiment was repeated using 10 ml of Zn<sup>2+</sup>, 15 ml of pH 10 buffer, and 5 drops of Eriochrome Black T indicator. The result of four such titrations is:

reading = 
$$3106^{\pm}4$$
  
blank =  $0029$   
volume =  $3077^{\pm}4$ 

To correlate the results:

$$\frac{3077^{\pm 4}}{10 \text{ ml}} \times \frac{42.31 \text{ in}}{6095} = 2.136^{\pm}0.003 \text{ in/ml}$$

Thus, there is excellent agreement between the two methods. It should be obvious that since this method is capable of precisely following very small changes even in highly conducting solutions, it makes possible conductometric analysis on other systems (such as redox reactions and ion exchange monitoring) in which it has previously been impossible or very impractical to make conductance measurements.

#### V. A NEW INSTRUMENT

#### A. Improvements

The prototype instrument worked so well that it was decided to build another instrument with many added features. In the new model, the pulse width is controlled by a 1 MHz crystal oscillator. This makes the pulse widths much more stable than the monostable multivibrator pulses used in the prototype. This, in turn, results in higher accuracy, since the pulses are much closer to being complementary. In addition, the pulses are only 10 µsec long for the shortest pulse width. Thus, the error due to polarization will be only half that of the prototype. The same crystal oscillator also controls the pulse repetition rate so that experiments may be carried out on a very accurate time scale.

As an additional improvement, 0.005% precision resistors are used so that a high absolute accuracy may be obtained. The offset current along with the sensitive null meter on this instrument allow it to make accurate measurements as a self-contained conductance "bridge" (with a linear, calibrated offset). The circuit was completely re-designed so the solid-state switch resistances no longer affect the accuracy. It can also operate with four cell leads so that all lead and contact resistances are unimportant.

Finally, an automatic temperature compensation circuit was added. This allows the temperature of the solution to vary by as much as 1°C without having a noticeable effect on the accuracy of the conductance readout. The output is automatically corrected to the value it would have had if the temperature of the solution had not changed.

#### B. The New Circuit

### 1. Analog Circuit

The block diagram of the new instrument is shown in Figure 14. The switches are in the positions as shown until condition A, B, or C exists, in which case, the appropriate switch changes state. The conditions occur as follows:

A - during the first pulse, B - during both pulses, and C - during the sampling time (the last 8/10 of the second pulse). The function of the operational amplifiers is given below.

All controls the top electrode of the cell to be precisely at +5  $R_2V/10~k\Omega$  during A and -5  $R_2V/10~k\Omega$  during the second pulse; i.e.  $\overline{A} \cdot B$  (" $\overline{A}$ " means "not the condition A" and "•" is the logical "and" symbol).

 $\underline{A2}$  furnishes an offset current to compensate for the cell current.  $R_1$  is a 100 kphm, 5 decade resistance box (0.005%). If  $R_1$  and  $R_3$  are adjusted so that the current from  $\underline{A2}$  is exactly opposite from the cell current at the end of condition B, then a "balanced-bridge" condition exists.

A3 provides an output voltage proportional to the conductance (with intercept determined by the offset current).

Figure 14

The Improved Bipolar Pulse Conductance Instrument

During C, A3 controls the bottom electrode to be at virtual ground and it charges the holding capacitor  $(C_h)$  so that at the end of the second pulse, the voltage across  $C_h$  is proportional to conductance. During  $\overline{C}$ ,  $C_h$  is connected to virtual ground, so that  $e_0$  remains proportional to the conductance.

 $\underline{A4}$  keeps the bottom electrode at virtual ground during  $\overline{C}$ . This further ensures complementary pulses, as was pointed out as necessary on page 46. A4 must sink the current supplied by A1 and A2 during  $\overline{C}$ .

A5 yields an output which is proportional to the total conductance (with an intercept of zero). This is used for temperature compensation.

 $\underline{A6}$  yields an output which is approximately proportional to the temperature deviation.  $R_T$  is a thermistor and  $R_A$  is the temperature adjustment. At the start of an experiment,  $R_A$  is adjusted to equal  $R_T$  ( $e_d = 0$ ). If the temperature changes,  $e_d$  will no longer be zero. This voltage and the output from A5 are multiplied together so that a temperature correcting current (which is proportional to the product of the conductance times the temperature deviation) is supplied to the summing amplifier, A3.

It is important to observe that the electrodes themselves are at precisely controlled potentials. The top electrode is connected to the inverting input of the voltage follower A1, and the lower electrode is connected to virtual ground of either A4 (durin,  $\overline{C}$ ) or A3 (during C). The outputs of the operational amplifiers control these inputs

(<u>via</u> the feedback loop) to be at the same potential as the non-inverting inputs (ground potential in the case of A3 and A4). Thus, both electrodes are controlled to be at precisely defined potentials regardless of switch, lead, contact, or cell resistance or inductance.

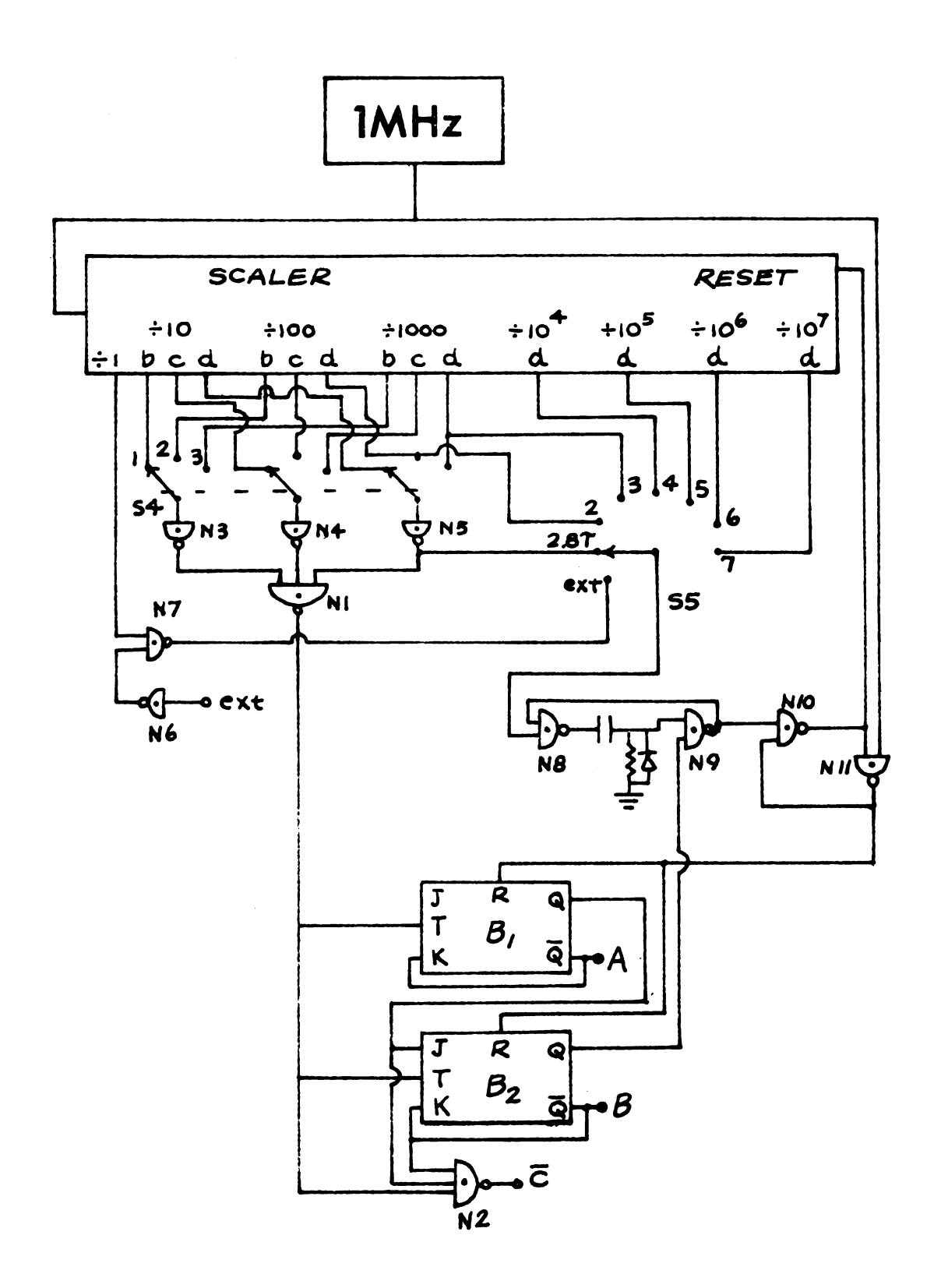
Amplifiers A1, A3, and A4 are very fast, settling to within 0.01% in 1  $\mu$ sec (69), so that rapid measurements can be made. The other amplifiers are not as fast, but since they are not involved with the pulses, speed is not a requirement. They do have low temperature drifts, so accuracy may be retained over a reasonable ambient temperature range. The multiplier has a rated accuracy of 1% and an output of  $\frac{e}{x} \sqrt{10V}$ .

# 2. Digital Circuit

The digital logic circuit is shown in Figure 15. The output of a 1 MHz crystal oscillator is scaled down to control both the pulse width (PW) and the pulse repetition frequency (PRF). The first three decades are used for the PW, and are gated so that the output of N1 is high during the last 8/10 of a period (the pulses are each one period long).  $B_1$  and  $B_2$  are LATCHED bistable multivibrators (J-K type), with the Q outputs going low only by resetting. The first low transition following resetting causes  $B_1$  to change states, but since the J input of  $B_2$  is connected to the Q output of  $B_1$ ,  $B_2$  will not change states until the second pulse. Since the K inputs are connected to the  $\overline{Q}$  outputs, the Q outputs cannot return to a low state (until reset). The logic levels A, B, and C are high during the first pulse, both pulses,

Figure 15

Digital Logic Circuit for Improved Instrument



and sampling time, respectively. These signals are converted to +5V/-15V levels in order to drive the switches.

N8 and N9 function as a gated reset monostable so that if the input from S5 to N8 goes low while logic  $\overline{B}$  exists, the reset cycle will start. The gated reset flip-flop (consisting of N10 and N11) then causes the scaler,  $B_1$ , and  $B_2$  to be reset. Notice that a new cycle cannot be started until the previous cycle is completed. When in the external trigger mode, N6 - N11 synchronize the trigger signal to the PW. Typical waveforms are shown in Figure 16 for the three trigger modes.

A complete circuit diagram, along with a further explanation of the components' functions and characteristics, is presented in the Appendix.

# C. Temperature Compensation

Assume that over a narrow temperature range the conductance of a solution and the conductance of a thermistor vary approximately linearly with temperature; i.e.

for the thermistor, 
$$G_T = \frac{1}{R_T} = \frac{1}{R_T^O} (1 + F_T \Delta T)$$
 (1)

and for the solution, 
$$G_{\mathbf{x}} = \frac{1}{R_{\mathbf{x}}} = \frac{1}{R_{\mathbf{x}}^{O}} (1 + F_{\mathbf{x}} \Delta T)$$
 (2)

where  $F_T$  and  $F_x$  are the temperature coefficients of conductance. From the block diagram in Figure 14,

$$e_{d} = \begin{pmatrix} \frac{5V}{R_{A}} & - & \frac{5V}{R_{T}} \end{pmatrix} \quad 500 \quad k\Omega$$

or 
$$e_d = -5V F_T \Delta T 500 k\Omega / R_T^O$$
 if  $R_A = R_T^O$  (3)

1			
-			

### Figure 16

# Waveforms of Logic Circuit

Logic Levels in Improved Instrument

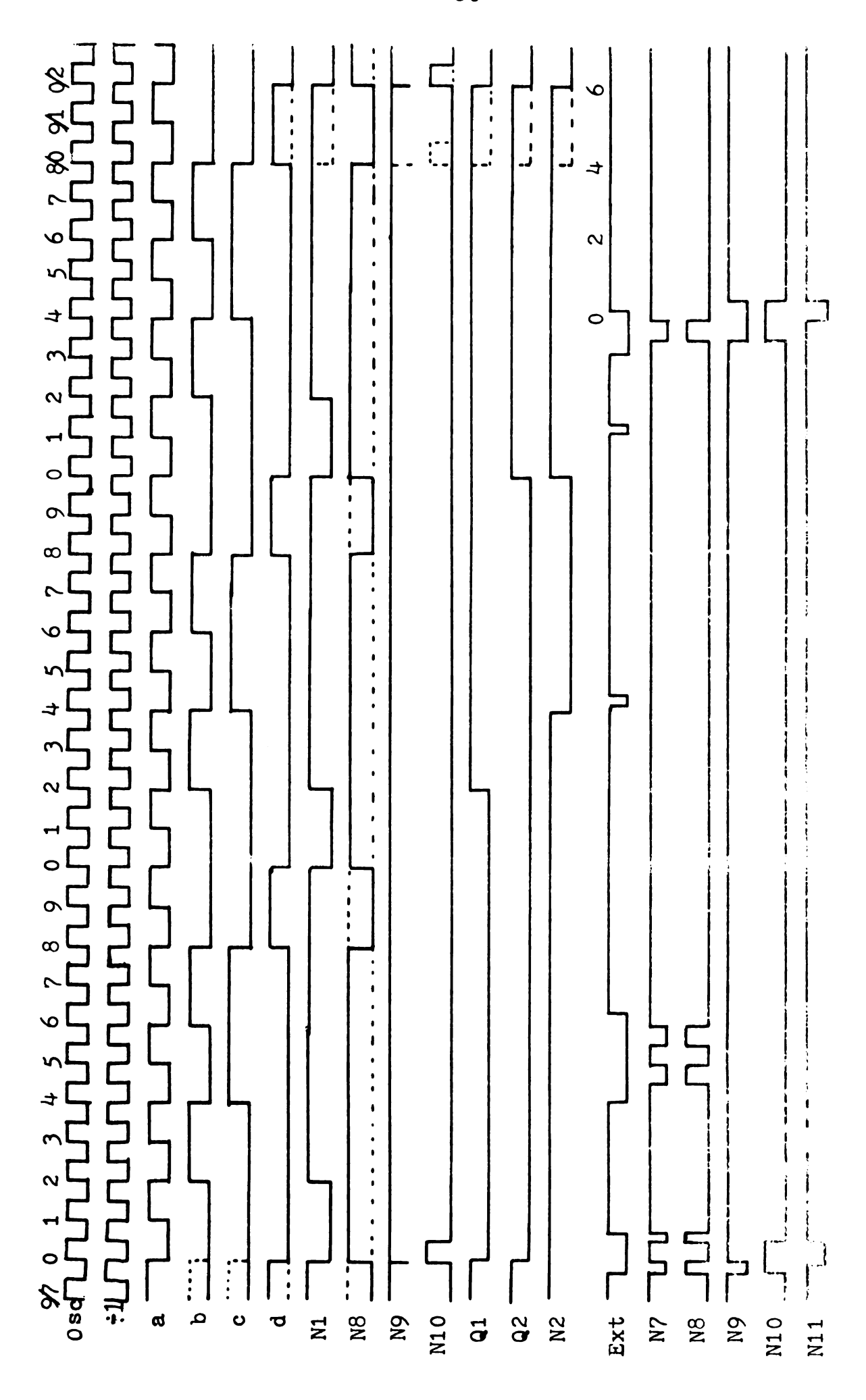
Pulse width setting is 10 µsec

Mode 1 = Pulse repetition on even decades

Mode 2 = Pulse repetition every 2.8 periods

(dashed lines)

Mode 3 = External triggering mode



<b>स</b> ्ट •			

Also, 
$$e_0 = -\left[\frac{e_d e_t}{10VR_6} + \frac{5V R_1}{100k\Omega R_3} - \frac{5V R_2}{10k\Omega R_x}\right] R_4$$
 (4)

and 
$$e_t = -\left[\frac{e_0}{R_4} + \frac{5V R_1}{100k\Omega R_3}\right] R_5$$

or 
$$e_t = \begin{bmatrix} \frac{e_d e_t}{10V R_6} - \frac{5V R_2}{10k\Omega R_x} \end{bmatrix} R_5$$
 (5)

Combining Equations 2, 3, and 5:

$$e_{t} = \left[ \frac{-5V F_{T} \Delta T 500 k \Omega e_{t}}{R_{T}^{0} 10V R_{6}} - \frac{5V R_{2}}{10k \Omega R_{x}^{0}} (1+F_{x} \Delta T) \right] R_{5}$$
 (6)

In order to have correct temperature compensation,

$$e_t = e_t^0 = \frac{-5V R_2 R_5}{10k\Omega R_x^0}$$
 (7)

Therefore, in order to have correct compensation, from Equations 6 and 7,

$$\frac{5V F_T \Delta T 500k\Omega e_t^o}{R_T^o 10V R_6} + \frac{5V R_2 F_x \Delta T}{10k\Omega R_x^o} = 0$$
 (8)

Combining Equations 7 and 8 again yields:

$$R_5 = \frac{2 R_T^0 R_6 F_x}{500 k\Omega F_T}$$
 (9)

Since  $R_6 = 5 k\Omega$ ,

$$R_5 = \frac{R_T^0 F_x}{50 F_m} \tag{10}$$

Therefore, from Equation 10 it is obvious that temperature compensation is possible providing that either the temperature coefficients are constant or that they vary in exactly

the same way. They should be nearly constant over a  $1^{\circ}$ C temperature range (the range for which this instrument was designed). The temperature adjustment is made by varying  $R_A$  (a 10 turn, 100 k $\Omega$  pot) until  $e_d$  is zero. At this point,  $R_A = R_T^0$ , so if the ratio of the temperature coefficients is known,  $R_5$  (a 10 turn, 2 k $\Omega$  pot) can be calculated directly. Armitage and French (70), however, have shown that it is very difficult to make an a priori temperature-coefficient prediction. In practice, therefore,  $R_5$  will be experimentally set by varying the temperature of the solution and adjusting  $R_5$  until  $e_0 = e_0^0$ .

### D. Obtaining Absolute Conductance

If proper compensation is made, the combination of Equations 2, 4, and 4 yields:

$$e_{o}^{o} = \frac{5V R_{4}}{100k\Omega} \left[ \frac{10 R_{2}}{R_{x}^{o}} - \frac{R_{1}}{R_{3}} \right]$$
 (11)

Equation 11 is the main equation for this instrument, as it allows the accurate determination of conductance. The voltage  $e_0$  is available at the front panel and also to the null meter. It is evident that if  $e_0 = 0$ , then:

$$\frac{1}{R_{\mathbf{x}}^{0}} = \frac{R_{\mathbf{1}}}{10 R_{2}R_{3}} \tag{12}$$

Therefore, this instrument can be used as a conductance "bridge" with no capacitance balancing. If the offset current is not used, the output,  $e_0$ , is a linear function of conductance with a zero intercept. If  $R_3 \neq \bullet$ , the intercept will change and a "bridge" with a linear off-balance is



obtained. Equation 11 can be written:

$$\frac{1}{R_{x}^{o}} = \left[\frac{100k\Omega e_{0}^{o}}{R_{4} 5V} + \frac{R_{1}}{R_{3}}\right] \frac{1}{10 R_{2}}$$
 (13)

Equation 13 suggests an extremely simple readout. Define five dimensionless variables:

$$a = R_1/10 \text{ k}\Omega$$
 (read one decade to the left of decimal point) 
$$b = 100 \text{ k}\Omega/R_3 = 100, 10, 1, 0 \text{ for } R_3 = 1, 10, 100, \text{ k}\Omega$$
 
$$c = 10 \text{ k}\Omega/R_2 = 100, 10, 1 \text{ for } R_2 = 0.1, 1, 10 \text{ k}\Omega$$
 
$$d = 200 \text{ k}\Omega/R_4 = 100, 10, 1 \text{ for } R_4 = 2, 20, 200 \text{ k}\Omega$$
 
$$e = e_0/1V$$
 (read output in volts)

Equation 13 then reduces to:

$$\frac{1}{R^0} = (ab + de)c \,\mu\Omega^{-1} \qquad (14)$$

#### E. <u>Instrument Tests</u>

#### 1. Absolute Accuracy

The absolute accuracy of the instrument was tested over its entire conductance range, using precision resistors in place of the cell. The results are summarized in Table 8.

There appears to be a systematic error that leads to a measured conductance which is approximately 0.02% low. The tolerance of the input resistor of A2 is temporarily only 0.01% (a 0.005% resistor will replace this resistor as soon as it arrives). The rest of the error can be attributed to the lack of optimization of the circuit. In the present work, for example, the amplifiers are over-compensated with

		,
		· · · · · · · · · · · · · · · · · · ·

TABLE 8

Absolute Accuracy Tests\*

R <sub>x</sub> (c	ohm)	Resistance Tolerance (%)	Measured G $(\mu\Omega^{-1})$	% Error
10		0.05	99,906	-0.094
50		0.01	19,998	-0.010
100		0.01	9.995.5	-0.045
500		0.01	1.999.4	-0.030
1	k	0.01	999•7	-0.030
5	k	0.01	199.96	-0.020
10	k	0.01	<b>99•</b> 98	-0.020
50	k	0.01	19.991	-0.045
100	k	0.01	9.9980	-0.020
500	k	1	2.0057	+0.285
1	M	1	1.0038	+0.380
5	M	1	0.1990	-0.500
10	M	1	0.0990	-1.000
30	M	1	0.0332	-0.400

Unless stated otherwise, all measurements were made with a pulse width of 1000 µsec and with the smallest "c" possible.

respect to high-frequency oscillation. This inhibits their response times and can cause error (especially for high  $R_4$  and short pulse widths). There is also the switching charge (the switching signal is coupled through the FETs capacitance to  $C_h$ ) which has not been fully compensated for in the sample and hold portion of the circuit. These problems are solvable, but their solution will take somewhat more time. Until the circuit is optimized, 0.05% absolute accuracy is all that can be claimed.

#### 2. Sensitivity

The sensitivity of this instrument was very good over its entire range. The limit of detection is shown in Table 9. (limit is = 0.1 scale division).

TABLE 9
Sensitivity vs. Resistance

Resista	ance $(\Omega)$	Detection of	1 part in
10		60,	000
100		200,	000
1	k	1,000,	000
10	k	100,	000
1.00	k	20,	000
1	M	8,	000
10	M	1,	000

The detection below  $1\,\mathrm{k}\Omega$  is limited by noise (the 50 mV and 0.5V pulses have relatively more noise than the 5V pulse). Above  $1\,\mathrm{k}\Omega$  the detection limit is due to the closed-loop gain of A3.

### 3. Dependence on the Parallel Cell Capacitance

The dependence on the parallel cell capacitance is shown in Table 10. These data were obtained using a resistance substitution box for  $R_{_{\scriptsize X}}$  and placing capacitors across the terminals.

From Table 10 it is obvious that the output is quite independent of  $C_p$ . There is some error as  $C_p$  increases, especially for large  $R_{\bf v}$ .

# 4. Dependence on Series Cell Capacitance

A series combination of a resistor and capacitor was used to determine the influence of the double-layer capacitance using this instrument. An ESI 0.01% decade resistance box was used for  $R_{\chi}$ . The results of this test are given in Table 11.

From these data, it can be seen that the dependence on  $C_{\mathbf{x}}$  is not large for small  $t/R_{\mathbf{x}}C_{\mathbf{x}}$ . It should be pointed out that the errors for small  $t/R_{\mathbf{x}}C_{\mathbf{x}}$  are probably due to the error in the measurement of  $R_{\mathbf{x}}$  (see Table 8) rather than the error caused by  $C_{\mathbf{x}}$ . Again, it should be pointed out that the largest capacitor tested is still much smaller than the typical  $C_{\mathbf{x}}$  of real cells.

### 5. Use of Four Cell Leads

The use of four cell leads to eliminate the influence of contact and lead resistance on the conductance measurement was explored. The conductance of two resistors was measured in three configurations: (1) with two leads, (2) with four normal leads, and (3) with a one ohm resistor in series with each lead. The results are listed in Table 12.

TABLE 10 Dependence on  $C_p$ 

	"a" -	term for bala	nce with C	in pF
$R_{x}(\Omega^{\pm}10\%)$	0	100	570	1070
l k	9.0324	9.0321	9.0322	9.0324
2.2 k	4.3352	4.3352	4.3354	4.3358
4.7 k	2.0529	2.0528	2.0528	2.0529
10 k	1.0253	1.0253	1.0254	1.0259
22 k	4.1332	4.1334	4.1335	4.1341
47 k	2.0137	2.0118	2.0097	2.0110
100 k	1.0370	1.0391	1.0380	1.0398
220 k	4.8760	4.8770	4.8784	4.8811
470 k	2.0280	2.0250	2.0272	2.0299
1 M	1.1071	1.1036	1.1064	1.1085
2.2 M	0.4330	0.4336	0.4350	0.4380
4.7 M	0.2290	0.2299	0.2310	0.2340
10 M	0.1089	0.1099	0.1110	0.1133

TABLE 11
Dependence on Series Capacitance

		measure	d G for C <sub>X</sub>	
R <sub>x</sub>	Theoretical G $(\mu\Omega^{-1})$	l µF	10 μF	
10	100,000	86,100	99,070	
50	20,000	19,220	19,996	
100	10,000	9,906	9,999	t = 10 µsec
500	2,000	1,998.3	1,999.8	
1000	1,000	999.8	999.91	
5000	200	199.96	199.92	
50	20,000	10,100	19,187	and analysis and analysis was after
100	10,000	8,200	9,910	
50 <b>0</b>	2,000	1,918.0	1,998.3	t = 100 µsec
1000	1,000	990.1	999•8	
5000	200	199.82	199.96	

TABLE 12
Elimination of Contact and Lead Resistance

Measured	G (	$(m\Omega^{-1})$
----------	-----	------------------

R <sub>x</sub>	Tolerance of $R_{\chi}$	2 Leads	4 Leads	4 Leads + $2\Omega$
10	0.05	99.904	99.907	99•9
50	0.01	19.998	19.999	20.0

Although the insertion of resistors in series with the leads reduced the sensitivity (because of noise), the fact that an accurate measurement can be made with a lead resistance that is 2/10 the value of  $R_{\chi}$  proves the value of the four-lead technique. It should be mentioned that long leads should be avoided unless proper compensation is provided to Al, A3, and A4; otherwise they are unstable.

### 6. A-C Bridge Comparison

The conductance of two solutions of KCl and of some conductivity water was measured using the bipolar pulse instrument and a Wayne - Kerr Bridge (Model # B 221). An experienced operator obtained the bridge measurements. The results are given in Table 13.

TABLE 13

A-C Bridge Comparison

Bipolar Pulse Techni	.que A-C	Bridge Technique
2.366 μΩ <sup>-1</sup>	(PW = 1000)	2.36 μΩ <sup>-1</sup>
11.295 μΩ <sup>-1</sup>	(PW = 1000)	11.30 μΩ <sup>-1</sup>
$2.8000  \mathrm{m}\Omega^{-1}$	(PW = 100)	2 795 m0 <sup>-1</sup>

### 7. Temperature Compensation

A variable temperature bath was set up to test the automatic temperature compensation. The temperature was varied by adjusting the ratio of hot to cold water flowing into the bath. The conductance of a KCl solution was followed vs. temperature with and without compensation. Without changing the temperature adjustment or the T.C. adjustment, more KCl was then added to the solution, and the experiment was repeated. The results are shown in Table 14.

From Table 14, it is obvious that temperature compensation by this method does work. The accuracy is increased by 1 - 2 significant figures. It should be noted that the zero temperature adjustment is slightly inaccurate in these examples. The temperature of the bath was easy to vary, but was very difficult to maintain at a constant temperature. Therefore, all adjustments (balance of A5 and the multiplier, adjustment of  $R_{A}$ , and the reading of the conductance with and without compensation) were not made with  $\Delta T = 0$ . This would not be a problem in a realistic situation, since the temperature would be constant. Although compensation was excellent for negative temperature deviations, it was not very good above a positive deviation of 0.25°C. Most likely the multiplier was not properly adjusted to obtain the best linearity for a large negative input signal (especially since  $\boldsymbol{e}_{t}$  is a small negative signal).

It is important to observe that the conductance and the temperature can both vary once proper adjustments are made. This is very important when following a reaction or a titration conductometrically.



TABLE 14
Temperature Compensation in KCl Solutions

Measured G ( $\mu\Omega^{-1}$ )(PW = 100  $\mu$ sec) <u>ΔΤ(°</u>C) With Comp. Without Comp. 4,851 -0.90 4,680 4.704 -0.754,853 -0.63 4,853 4.726 -0.50 4,853 4,751  $T = 14.5^{\circ}C$ 4,854 4.802 -0.25 4.847 0.00 4.852 0.25 4,853 4,896 0.50 4,867 4,940 4,887 4,988 0.60 -1.25 5,492 5,195 -1.00 5,491 5,271 -0.755,494 5,323 5,376 -0.50 5,496 -0.25 5,493 5,438 -0.12 5,493 5,456 Temp. adj. and T.C. adj. remain 0.00 5,492 5.484 the same. 1.25 5,493 5,540 More KCl added. 0.50 5,503 5,590 0.75 5,525 5,646 0.90 5,542 5,680

#### VI. CONCLUSION

The bipolar pulse technique makes many experimental parameters non-critical or at least not as critical as when using a-c or d-c techniques. The method is unique in that it combines all of the desirable features of high and low frequency a-c techniques while making the actual measurement using a d-c potential. Most of the limitations of the traditional techniques are eliminated or reduced to a tolerable level. The most important advantage of this technique is its relative independence of all cell capacitances.

Since this technique is independent of  $\mathbf{C}_p$ , accurate conductance measurements can be made in solutions of low conductance. The cell design and lead length are no longer critical. Since the Parker effect is eliminated, oil baths are not needed. This technique should prove extremely useful when working with non-aqueous solutions.

Since this technique is not strongly dependent on C<sub>X</sub>, many experimental difficulties are eliminated. Platinization is not necessary. Therefore, many new chemical systems, in which surface adsorption on platinized platinum is a problem, may be studied conductometrically. It is also possible to use small electrodes. This makes possible conductometric determinations using small cells (such as would be used for a conductivity detector in ion-exchange). This also has

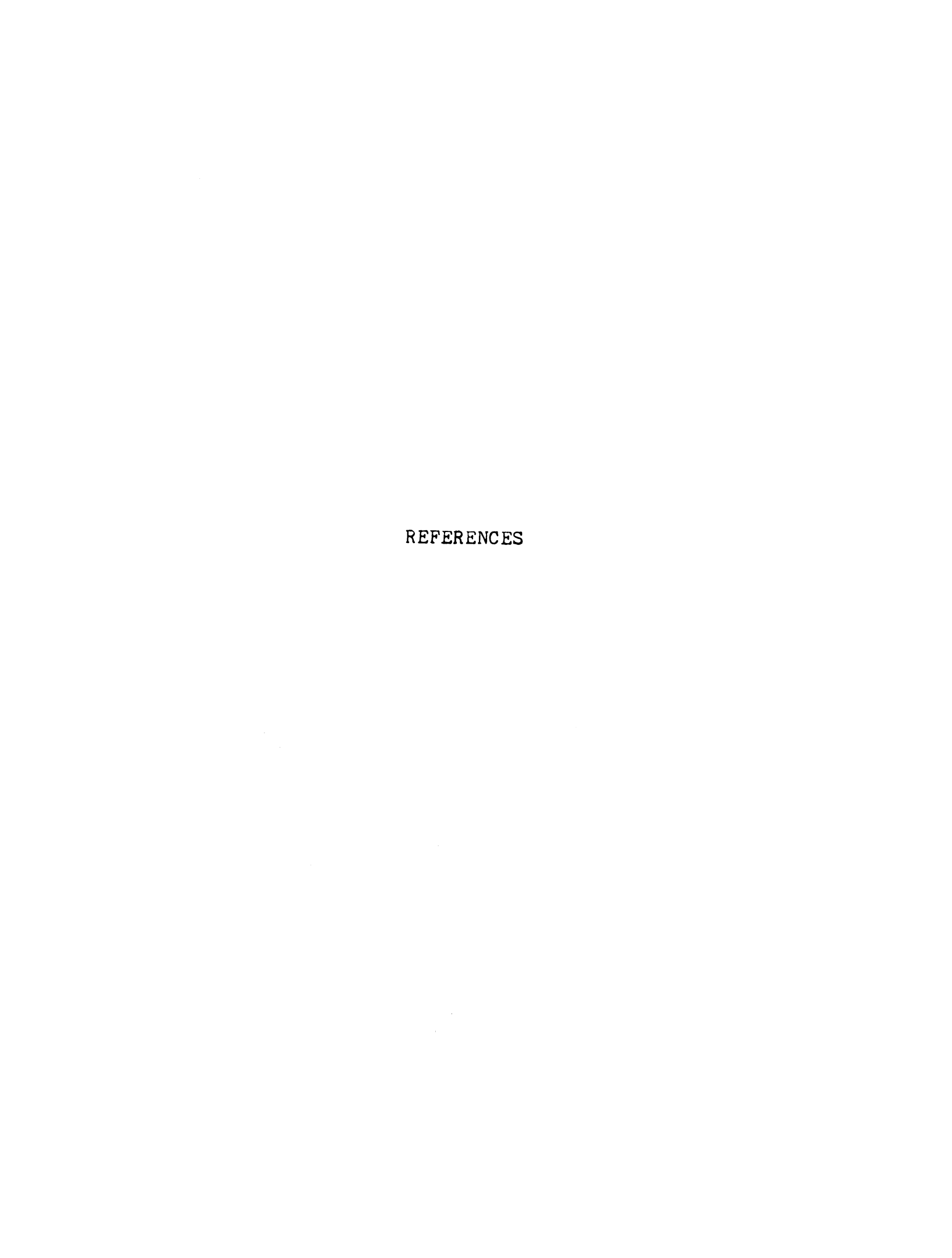
application in the bio-medical field, such as in the study of  $Na^+/K^+$  exchange in nerves and blood. The lack of dependence on  $C_{\mathbf{x}}$  also permits accurate measurements on very high conductance solutions (such as molten salts).

Independence of the cell capacitances has several other advantages. The time-consuming bridge balance is not necessary (bridge balance also requires a pure signal with no harmonics, as the capacitive reactances are only balanced at one frequency). This permits very rapid conductance measurements. Rapid measurements with small electrodes are very useful for fast kinetic studies (such as stopped-flow). The bipolar pulse technique is also readily applicable to other flow systems which require continuous monitoring, such as ion-exchange or liquid-liquid chromatography. It may even be possible to detect non-conducting liquids by injecting a continuous flow of ions into the effluent stream. As the non-conducting liquid comes off the column, it may change the dielectric constant of the effluent and/or the solvation spheres of the ions enough to detect a change in conductivity (recall a sensitivity of up to 1 ppm).

The circuit of the bipolar pulse instrument permits compensation for various experimental parameters. The temperature compensation circuit of the new instrument is just one example. Another example is the application of a current ramp to the summing point of the output amplifier in order to compensate for a linearly increasing (or decreasing) conductance. This was done using the prototype instrument to follow the change in slope during a titration. This

technique may allow conductance to be used to follow titrations in which the number of ions is unchanged, but in which the ions undergo a change in solvation number (or in which ions of similar, but not equal, equivalent conductance are exchanged).

In summary, the bipolar pulse technique can be used under any conditions that traditional techniques can be used (including the accurate determination of cell constants and equivalent conductance). In addition, it can be used in many circumstances that the traditional techniques cannot be used. This technique is extremely simple to use, as it requires no balancing, and the output is directly proportional to the conductance. In addition, very rapid measurements may be made. Thus, this technique should prove to be very useful for the accurate determination of conductance under a wide variety of experimental conditions.



### REFERENCES

- 1. Newberry, E. J. Chem. Soc. 113, 701 (1918).
- 2. Eastman, E. J. Am. Chem. Soc. 42, 1648 (1920).
- 3. Kraus, C. and Fuoss, R. <u>J. Am. Chem. Soc.</u> <u>55</u>, 21 (1933).
- 4. Gunning, H. and Gordon, A. <u>J. Chem. Phys.</u> <u>10</u>, 126 (1942).
- 5. Elias, L. and Schiff, H. <u>J. Phys. Chem.</u> 60, 595 (1956).
- 6. Gavis, J. J. Chem. Phys. 41, 3787 (1964).
- 7. Jaffe, G. and LeMay, C. J. Chem. Phys. 21, 920 (1952).
- 8. Douwes, C. and van der Waarder, M. J. Inst. Petrol. 53, 237 (1967).
- 9. Kohlrausch, F. Wied. Ann. 49, 249 (1893).
- 10. Kohlrausch, F. and Holborn, L. <u>Das Leitvermögen Der Elektrolyte Insbersondere Der Lösungen.</u> Beipzig: B. G. Teubner, 1898.
- 11. Washburn, E. and Bell, J. <u>J. Am. Chem. Soc.</u> <u>35</u>, 17? (1913).
- 12. Washburn, E. J. Am. Chem. Soc. 38, 2431 (1916).
- 13. Hall, R. and Adams, L. <u>J. Am. Chem. Soc.</u> 41, 1515 (1919).
- 14. Gieringer, C. Rev. Sci. Instr. 7, 414 (1936).
- 15. Jones, G. and Josephs, R. <u>J. Am. Chem. Soc.</u> 50, 1049 (1948).
- 16. Taylor, W. and Acree, S. <u>J. Am. Chem. Soc.</u> 38, 2403 (1916).
- 17. Jones, G. and Bollinger, G. <u>J. Am. Chem. Soc.</u> <u>51</u>, 2407 (1929).

- 18. Jones, G. and Bollinger, G. <u>J. Am. Chem. Soc.</u> <u>53</u>, 411 (1931).
- 19. Parker, H. J. Am. Chem. Soc. 45, 1366, 2017 (1923).
- 20. Randall, M. and Scott, G. <u>J. Am. Chem. Soc.</u> 49, 636 (1927).
- 21. Smith, F. J. Am. Chem. Soc. 49, 2167 (1927).
- 22. Shedlovsky, T. J. Am. Chem. Soc. 52, 1793 (1930).
- 23. Foy, W. and Martell, A. Rev. Sci. Instr. 19, 628 (1948).
- 24. Cole, R. and Gross, P. Rev. Sci. Instr. 20, 252 (1949).
- 25. Hladek, L. Chem. Listy 60, 238 (1966).
- 26. Warburg, E. Wied. Ann. Physik. 67, 493 (1899).
- 27. Winterhager, H. and Werner, L. <u>Forschungsber.</u> des Witschafts. No. 341 (1956).
- 28. Feates, F., Ives, D., and Pryor, J. <u>J. Electrochem.</u> <u>Soc.</u> 103, 580 (1956).
- 29. Metcalf, W. J. Sci. Instr. 42, 742 (1965).
- 30. Robbins, G. and Braunstein, J. <u>J. Electrochem. Soc.</u> <u>116</u>, 1218 (1969).
- 31. Bertram, R. and Cruse, K. Ber. Bunsenges. Physik. Chem. 67, 98 (1963).
- 32. Bertram, R. and Cruse, K. Z. Anal. Chem. 186, 213 (1962).
- 33. Cruse, K. and Bahr, E. Z. Anal. Chem. 197, 141 (1963).
- 34. Wershaw, R. and Goldberg, M. <u>Anal. Chem.</u> <u>37</u>, 1180 (1965).
- 35. Warshawsky, I. Rev. Sci. Instr. 26, 711 (1955).
- 36. Griffiths, V. Talanta. 2, 230 (1959).
- 37. Griffiths, V. Anal. Chim. Acta. 18, 174 (1958).
- 38. Ferris, C. Rev. Sci. Instr. 34, 109 (1963).
- 39. Hanss, M. and Guermonprez, R. <u>J. Chim. Phys.</u> <u>63</u>, 663 (1966).

		· · · · · · · · · · · · · · · · · · ·
igst		
· . 		

- 40. Janz, G. and McIntyre, J. J. Electrochem. Soc. 108, 272 (1961).
- 41. Walisch, W. and Barthel, J. <u>Z. Physik. Chem.</u> <u>34</u>, 38 (1962).
- 42. Walisch, W. and Barthel, J. Z. Physik. Chem. 39, 235 (1963).
- 43. Schmidt, K. Rev. Sci. Instr. 47, 671 (1966).
- 44. Robertson, R. Can. J. Chem. 33, 1536 (1955).
- 45. Robertson, R. and Hyne, J. Can. J. Chem. 35, 623 (1957).
- 46. Murr, B. and Shiner, V. <u>J. Am. Chem. Soc.</u> <u>84</u>, 4672 (1962).
- 47. Sirs, J. Trans. Faraday Soc. 54, 201 (1958).
- 48. Prince, R. Trans. Faraday Soc. 54, 838 (1958).
- 49. Strehlow, H. and Wendt, H. Inorg. Chem. 2, 6 (1963).
- 50. Eurato, E. and Leimu, R. <u>Acta. Chem. Scand.</u> 20, 2029 (1966).
- 51. Dusek, K. and Lesek, J. Chem. Listy. 59, 1353 (1965).
- 52. Tregloam, P. and Laurence, G. <u>J. Sci. Instr.</u> <u>42</u>, 869 (1962).
- 53. Mori, I. and Chikui, S. J. Chrom. 20, 627 (1965).
- 54. Duhne, C. and Sanchez, O. Anal. Chem. 34, 1074 (1962).
- 55. Pecsoc, R. and Saunders, D. Anal. Chem. 40, 1756 (1968).
- 56. Pecsoc, R. and Saunders, D. Anal. Chem. 40, 44 (1968).
- 57. Knudson, G., Ramaley, L. and Holcombe, W. Chem. Instr. 1, 325 (1969).
- 58. Gerischer, H. Z. Elektrochem. 58, 9 (1954).
- 59. Cruse, K. Z. Chem. 5, 1 (1965).
- 60. Barthel, J. Angew. Chem. Int. Ed. 7, 260 (1968).
- 61. Fuoss, R. and Accascina, F. <u>Electrolytic Conductance</u>. New York: Interscience Publishers, Inc., 1959.
- 62. Davies, C. <u>Ion Association</u>. London: Butterworths, 1962.

			1
			!
			1
			1
			) )
			+
9 9			
			,

- 63. Monk, C. <u>Electrolytic Dissociation</u>. New York: Academic Press, 1961.
- 64. Nancollas, G. <u>Interactions in Electrolyte Solutions</u>.

  New York: <u>Elsevier Publishing Co.</u>, 1966.
- 65. Thompson, H. and Rogers, M. Rev. Sci. Instr. 27, 1079 (1956).
- 66. Lund, H. and Bjerrum, J. Ber. B64 210 (1931).
- 67. Hartley, H. <u>Technometrics</u> 3, 269 (1961).
- 68. Daum, P. Ph. D. Thesis, Mich. State Univ., East Lansing, Michigan (1969).
- 69. Analog Devices. A Selection Handbook and Catalog Guide to Operational Amplifiers. (1969).
- 70. Armitage, P. and French, C. J. Chem. Soc. 1963, 743.



· ·			
اً المع			

## APPENDIX A

PROGRAM FOR CALCULATING PSEUDO FIRST-ORDER RATE CONSTANTS

The general equation for the pseudo first-order rate constant is:

$$\frac{C_{\infty} - C_{t}}{C_{\infty} - C_{0}} = \exp(-kt) \tag{1}$$

where C is the concentration at time 0, t, and ∞, and k is the rate constant.

If the conductance is proportional to concentration, Equation 1 becomes:

$$\frac{G_{\bullet} - G_{t}}{G_{\bullet} - G_{0}} = \exp(-kt)$$
or  $G_{t} + (G_{\bullet} - G_{0}) \exp(-kt) - G_{\bullet} = 0$  (2)

A computer program was written to minimize the equation:

$$E = \sum_{i=1}^{n} \left[ Y_i + B \cdot \exp(-kX_i) - A \right]^2$$
 (3)

where Y<sub>i</sub> = the i<sup>th</sup> conductance reading

X; = the i<sup>th</sup> time reading

 $A = G_{\infty}$ 

 $B = G - G_0$ 

Equation 3 is differentiated with respect to each curve-fit variable, A, B, and k. The partial derivitive in each case is set equal to zero and a value for  $\Delta A$ ,  $\Delta B$ , or  $\Delta k$  is

calculated:

$$\Delta A = \frac{n}{\sum_{i=1}^{n} \left[ Y_i + B \cdot \exp(-kX_i) - A \right]}$$
 (4)

$$\Delta B = -\frac{\sum_{i=1}^{n} \exp(-2kX_{i})}{\sum_{i=1}^{n} \exp(-kX_{i})[Y_{i} + B \cdot \exp(-kX_{i}) - A]}$$
(5)

$$\Delta k = \frac{\sum_{i=1}^{n} X_{i}^{2} \exp(-kX_{i})[Y_{i} + 2B \cdot \exp(-kX_{i}) - A]}{\sum_{i=1}^{n} X_{i} \exp(-kX_{i})[Y_{i} + B \cdot \exp(-kX_{i}) - A]}$$
(6)

Since A, B, and k are not independent variables, the whole difference cannot be used as it can with the simple Newton successive approximation. It is assumed that the least squares error, E, as calculated from Equation 3 is a parabolic function of the fraction, v, defined by the equations:

$$A_{j+1} = A_j + v\Delta A$$
 (the (j+1)<sup>th</sup> iterative value of A) (7)  
(v is a fraction between 0 and 1)  
 $B_{j+1} = B_j + v\Delta B$  (8)

$$k_{j+1} = k_j + v\Delta k \tag{9}$$

The optimum v occurs at the minimum of the parabola and is:

$$v_{op} = \frac{(4 E_{\frac{1}{2}} - 3 E_{o} - E_{\frac{1}{2}})}{4 (E_{\frac{1}{2}} + E_{o} - 2E_{\frac{1}{2}})}$$

where 
$$E_0 = E$$
 when  $v = 0$ 

$$E_{\frac{1}{2}} = E$$
 when  $v = \frac{1}{2}$ 

$$E_1 = E$$
 when  $v = 1$ 

₹ 4 . '  			

The new values of A, B, and k are then calculated from Equations 7 - 9 with  $v = v_{op}$ . As soon as the values do not change by more than the quitting tolerance, the iterative procedure halts.

Table A-1 shows the three-parameter, least-squares, curve-fit program which was written to obtain the results listed in Table 7. It was written for a PDP 8/i computer, but could easily be modified for other computers.

As written, there are three independent options for operation, depending on the code that is typed:

odd code = type log plot using final values

code < 5 = print values after each iteration

2 < code < 7 = pause after each set of data
Thus, the input data necessary is:</pre>

- (1) the experiment name or number
- (2) the number of seconds in each time interval

first line

- (3) the infinite conductance
- (4) the iteration stopping tolerance (%)
- (5) time

succeeding lines

(6) conductance

(7) time = -1.0 end of data

Typical input and output is shown in Table A-2.

## TABLE A-1

## THREE-PARAMETER, LEAST-SQUARES, CURVE-FIT PROGRAM

```
C THIS PROGRAM CALCULATES A FIRST ORDER RATE CONSTANT FOR ANY
   PROPERTY WHICH IS PROPORTIONAL TO CONCENTRATION.
 C A 3-PARAMETER LEAST SQUARES CURVEFIT IS DONE.
DIMENSION X (25), Y (25), Q (3)
          READ (1.108) K1
FORMAT ('CODE = '12)
 108
          K4=1
          IF (X1)21,21,22
21
          K4=8
          K3=(K1-3)+(K1-6)
22
          K2=K1-2+(K1/2)
          K1=K1-5
          READ (2, 101) ALPH, TM, FL, TOL
101
          FORMAT (A6,2X3F8.3)
          TOL=(.01+TOL)++2
          I = 0
12
          I = I + 1
          READ (2,103)X(I),Y(I)
103
          FORMAT (2F8.3)
          X(I) = X(I) * TM
          IF (X(I)) 13,12,12
13
          N= I - 1
          FN: N
          VX = 0
          IF (FL)3,4,4
3
          1=0
         X2=(X(N)-X(1))/2.
         I = I + 1
         IF (X2-X(I))6,6,5
6
         12=1-1
         Y2=Y(I)-(Y(I)-Y(I2))*(X(I)-X2)/(X(I)-X(I2))
FL=Y2+(Y2-Y(I))*(Y(N)-Y2)/(2.*Y2-Y(I)-Y(N))
         G=ALOG((FL-Y(1))/(FL-Y(N)))/(X(N)-X(1))
         B=(FL-Y(1))*EXP(G*X(1))
15
         S1=0
         S2=0
         S3=0
         S4=0
         55=0
C SUMMING ROUTINE
         DO 50 I=1,N
T=X(I)
         A=EXP(-G+T)
         H=Y(I)+B+A-FL
```

S1 = S1+H

<b>-</b> 80			

## TABLE A-1 (continued)

```
S2:S2+A+H
         53=53+A**2
         S4=S4+T++2+A+(H+A+B)
50
         S5=S5+T*A+H
         IF (KI)32,33,33
         WRITE (1,200) FL.G.B.VX
FORMAT (3E12.6,F5.3)
32
200
         DL=.5+S1/FN
33
         DB=-.5+52/S3
         DK=.5+S5/S4
C CONVERGENCE GUARANTEE
         DO 40 J=1,3
         SS=0
         DO 39 I=1.N
39
         SS=SS+(Y(1)+B+EXP(-G+X(1))-FL)++2
         Q(J)=SS
         B:B+DB
         G=G+DK
40
         FL = FL+DL
         V=-.5+(4.+Q(2)-3.+Q(1)-Q(3))/(Q(3)+Q(1)-2.+Q(2))-3.
         VX=(V+3.)/2.
         G=G+V+DX
         FL=FL+DL+V++K4
         B=B+V*DB
  TEST FOR CONVERGENCE
C
         IF ((DK/G)++2-TOL)34,15,15
IF ((DL/FL)++2-TOL)35,15,15
35
         IF ((DB/B)++2-TOL)36,15,15
36
         SS=0
         DO 26 I=1.N
         SS=SS+(Y(1)+B+EXP(-G+X(1))-FL)++2
26
         SC=100.+(SS/(FN-1.))++.5/(Y(N)-Y(1))
         WRITE (1,100) ALPH, G, FL, SC
FORMAT (A6, ' K= ' E12.6, ' INF G = ' F10.6, ' SCAT = 'F7.3, ' Z')
100
         IF (K2)61,61,59
         WRITE (1,126)
FORMAT ( T
106
                       TIME
                                    LN(GI-G)')
         DO 60 I=1.N
         FN=ALOG(FL-Y(I))
         WRITE (1,107)X(1),FN FORMAT (2(1XF13.4))
60
137
         IF (K3)1,1,62
61
         PAUSE
62
         GO TO 1
         END
```

INPUT AND OUTPUT OF LEAST-SQUARES PROGRAM

TABLE A-2

A1.1	2.0	7457•	0.01
6.	4150.		
9•	5297.		
12.	6041.		
15.	6529.		
18.	6847.		
21.	7056.		
24.	7194.		
27.	7282.		
30.	7339.		
33.	7377		
36.	7403.		
39.	7420.		
42.	7430.		
-1.	0.		
- •	- <b>-</b>		

A1.1 INFIN G = 7457.000

-5.8785

84.0000

K= •707209E-01 INFIN G = 7463.2 SCAT = .052% 1 TIME LN(GI-G) 12.0000 -.8150 18.0000 -1.2419 24.0000 -1.6657 30.0000 -2.0905 36.0000 42.0000 -2.5135 -2.9383 -3.3683 48.0000 -3.7878 54.0000 60.0000 -4.1996 66.0000 -4.6146 72.0000 -5.0484 -5.4871 78.0000

## APPENDIX B

# CIRCUIT DESCRIPTION OF IMPROVED BIPOLAR PULSE CONDUCTANCE INSTRUMENT

The circuit diagram of the analog portion is shown in Figure B-1. A description of each critical component is given below.

The -5V reference supply is an integrated circuit voltage regulator (LM 304, made by National Semiconductor). Its rated accuracy is 0.01%.

The resistors from -5V to ground and to A2 have tolerances of 0.005%, as do the resistors from A2 and A3 to the summing point (bottom electrode of cell). The feedback resistance of A2 is a 5 decade, 100 k $\Omega$  resistance sub-assembly with a rated accuracy of 0.005%. All of these are metal film resistors and have temperature coefficients of 1 ppm/C $^{\circ}$ . These resistors have very low capacitances, having rise-times of less than 1 nsec. They are the only resistors involved with the actual pulses.

A3 and A4 are very fast (to 0.01% in 1 µsec) differential amplifiers (Analog 148B). Their common-mode rejection ratio (CMRR) is not very high, but since the non-inverting input is grounded, the CMRR is unimportant.

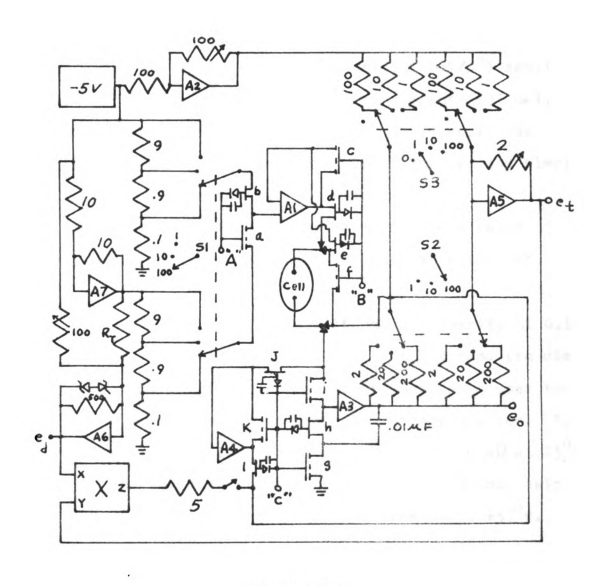


Figure B-1
CIRCUIT DIAGRAM OF THE IMPROVED CONDUCTANCE INSTRUMENT

(All resistances in kohm)

They have low input currents (necessary for sample and hold) and up to 20 mA of output current. A4 must sink all of the current coming to the summing point during  $\overline{C}$ .

Al (149B) has similar specifications to A3 and A4, but it also has a high CMRR (15,000). This is necessary since it functions as a voltage follower.

A2, A5, and A6 (119K) are low drift (5 uV/C°) amplifiers. They have relatively high input currents (35 nA), but they are not used in any portion of the circuit that would be affected by this current. A7 (142B) is used simply as an inverter and is not at all critical.

The multiplier (Hybrid Systems 107C) has a rated accuracy of 1% over four quadrants and has an output of  $e_x e_y/10V$ .

The 100 k $\Omega$  pot (10 turn) to A6 has a linearity of 0.1%. There is a 10 k $\Omega$  l% resistor in series with it, and the dial reads from 10 k $\Omega$  to 110 k $\Omega$ . This potentiometer is used to adjust for temperature during temperature compensation.  $R_T$  is a thermistor (YSI, 1%) with a resistance of 30 k $\Omega$  at 25°C. Without adding any more resistance to the 100 k $\Omega$  pot, this thermistor permits temperature balance from -4 to +52°C.

The feedback resistance of A5 is a 2 k $\Omega$ , 10 turn pot (0.1% linearity). It is used to adjust the temperature coefficient (see Equation 10 on page 81). The feedback resistance of A6 and the output resistance (5 k $\Omega$ ) of the multiplier have a 1% tolerance. All previously undefined resistance are 0.1%. The 10.2V zener diodes across A6 prevent it from limiting when the temperature is unbalanced.

Switch 1 is a non-critical three-position switch (it may have high contact resistance since no current flows through it). Switches 2 and 3 are high-quality switches with silver contacts since they must have resistances which are negligible with respect to 1 k $\Omega$  (S3) or 2 k $\Omega$  (S2).

The transistor switches (a-1) are driven by the output of a Fairchild 9624 interface gate (which converts a + 5V input to -15V, and a OV input to +5V as used in this instrument). All six of the N-channel junction FETs are TIS73 transistors. A gate signal of -3V turns them "off". The P-channel, enhancement mode MOS-FETs (a, c, f, g, i, and k) do not turn "on" until the gate signal is -6V. Since all of the gates in each set of transistors are driven by the same signal, a "break-before-make", single, double, or triple pole, double-throw switch is obtained when driven by "A", "B", or "C", respectively. During condition A (see page 75), "A" is -15V, during condition B, "B" is at +5V, and during condition C, "C" is at -15V. The choice of logic level to use is explained as follows.

Transistor "a" is further "on" if connected to +5V rather than -5V, and Al has to be connected to the minus voltage during the second pulse. Therefore, "A" must be -15V.

The N-channel FETs have a much lower "on" resistance than do the P-channel FETs. It is desirable, therefore, to have transistors d and e "on" during condition B. Thus, "B" = +5V.

Amplifier A4 must sink considerable current (up to 10 mA) during  $\overline{C}$ . Therefore, the P-channel transistors are

"on" during C (they have an 8 mA rating).

Notice that the "on" resistances of transistors a, b, c, e, i, j, and k are not critical since no current flows to the inputs of the operational amplifiers. As long as the amplifiers are functioning, the electrodes themselves are the controlled points, since they are connected to the inverting inputs of Al and either A3 (during C) or A4 (during  $\overline{C}$ ) by transistors e, i, and j, respectively.

The 0.01  $\mu F$  holding capacitor is connected to ground during C and to virtual ground during  $\overline{C}$ . Thus, e remains (during  $\overline{C}$ ) at the voltage that is proportional to the conductance.

 $e_t$  is proportional to the total conductance (with zero intercept). This value is multiplied by the temperature deviation in order to feed a temperature-correcting signal to A3 that is proportional to the product  $G\Delta T$ .

It should be mentioned that separate signal and power grounds (connected at a common point) were used. Also, separate power supplies were used for the amplifiers involved with the pulses and those working at d-c. The analog portion is covered with a metal shield and is completely separate from the +5V digital logic supply.

The digital portion of this instrument consists of:

- (1) a Heath EU 800 27 crystal oscillator card
- (2) a Heath EU 800 28 7-decade scaler card
- (3) a card consisting of:
  - (a) two SN7400N quad, 2-input NAND gates
  - (b) one SN7410N triple, 3-input NAND gate
  - (c) a SN7476N Dual J-K Flip-flop
  - (d) the interface gates (switch drivers)

A picture of the front panel is shown below.



Figure B-2
The Bipolar Pulse Instrument Front Panel

The instrument panel has been arranged for the convenient measurement of conductance. The pulse width should be adjusted for the conductivity of the solution with a rough guide being:

PW = 10  $\mu$ sec for G > 1  $m\Omega^{-1}$ 

PW = 100 µsec for  $1 \text{ m}\Omega^{-1} > G > 0.1 \text{ m}\Omega^{-1}$ 

PW = 1000 µsec for  $G < 0.1 \text{ m}\Omega^{-1}$ 

Normally the pulse repetition frequency is at least ten times the  $PW_{\bullet}$ 

The maximum cell current is 5 mA. The "c" switch (lower right) controls the pulse amplitude to be consistent with this current.

c = 100 (v = 50 mV) for 
$$10 \Omega < R_x < 100 \Omega$$
  
c = 10 (v = 500 mV) for  $100 \Omega < R_x < 1 k\Omega$   
c = 1 (v = 5V) for  $R_x > 1 k\Omega$ 

The lower the pulse voltage, the higher will be the relative noise-level, so that unless  $C_{\chi}$  is small (so that  $Z_{F}$  might be important), the highest voltage that provides under 5 mA should be used. One should begin with c = d = 100 and decrease c until "e" is between one and ten volts.

Then "a" (the feedback resistor of A2) and "b" (the offset multiplier) are adjusted until e = 0. The output amplifier (A3) gain may then be increased (d decreased), and "a" readjusted. The meter may also be made more sensitive in order to achieve very sensitive balance.





		-

